

## Space-Time Correlations in Anisotropic Heisenberg Paramagnets at Elevated Temperatures

DANIEL G. McFADDEN\*† AND RAZA A. TAHIR-KHELI‡

*Department of Physics, Temple University, Philadelphia, Pennsylvania 19122*

(Received 28 August 1969)

The structure of the space-time-dependent spin-correlation functions for an anisotropic Heisenberg paramagnet with cylindrical symmetry at elevated temperature is analyzed in terms of a two-parameter Gaussian representation of the generalized diffusivity. The parameters are chosen so as to exactly preserve the frequency moments, i.e.,  $\langle \omega^{2n} \rangle_{\mathbf{K}}^{\alpha\alpha}$  ( $\alpha = z, x, \text{ or } y; n = 0, 1, 2$ ) of the longitudinal and the transverse spectral functions. These moments are calculated for arbitrary spin  $S$ , arbitrary range of the exchange interactions, and arbitrary dimensionality. The results for the correlation functions are worked out for one, two, and three dimensions. In the extreme transverse limit, the results are compared with the exactly soluble  $XY$  model for a one-dimensional spin- $\frac{1}{2}$  system with only nearest-neighbor (transverse) exchange. The agreement of the results is found to be satisfactory.

### I. INTRODUCTION

IN exchange-coupled spin systems, the static, i.e., time-independent, correlation functions can be determined to a high degree of accuracy in the paramagnetic phase. The relevant computational procedures, which rely on the development of appropriate high-temperature series expansion of the equilibrium density matrix, have now reached a great degree of sophistication. Indeed, these computations have even led to an understanding of the structure of the most involved of all the many-body phenomena, i.e., the cooperative phase transition.<sup>1</sup>

The state of the knowledge of the time-dependent paramagnetic correlation functions is, however, an entirely different story. Except for a few exceptions (to be enumerated below), no reliable solutions of the dynamical correlations can be obtained even in the limit of extremely high temperatures.

Since the writing of the classic work of Kubo and Tomita,<sup>2</sup> several recent calculations have pioneered the study of the time dependence of the spin-correlation functions. The first of these calculations<sup>3</sup> considers a finite sample ( $N \sim 10^3$ ) of classical spins coupled by isotropic nearest-neighbor (nn) Heisenberg exchange at infinite temperature and numerically charts their development in time on an electronic computer. The results then are interpreted in the thermodynamic limit, i.e.,  $N \rightarrow \infty$ . Because no essential theoretical approximations are introduced into these calculations (except for those related to numerical computations), for the present purposes, we shall regard these results as being "exact."

The second set of calculations<sup>4</sup> deal with a small linear array of quantum spins of magnitude  $\frac{1}{2}$  (we shall use Dirac's units where  $\hbar = 1$ ) which are coupled by isotropic nn Heisenberg interactions. Here, the time dependence is painstakingly evaluated by determining the relevant eigenfunctions and eigenvalues of small clusters, i.e.,  $N = 6, \dots, 10$ , of spins, using this information in the infinite-temperature density matrix and finally by carrying out plausible extrapolation of these results to the thermodynamic limit  $N \rightarrow \infty$ . Again, for the present purposes, we shall refer to those results as being exact.

The third set of such exact calculations (which are probably the earliest ones carried out<sup>5</sup>) also deal with a finite assembly of classical Heisenberg spins whose behavior is numerically charted out.<sup>6,7</sup> However, in this paper, unlike Ref. 3, the initial conditions are chosen for various ranges of temperature by the Monte Carlo technique in such a way that self-consistency between the static and the time-dependent results is achieved for the temperature in question.

In addition to the aforementioned computer experiment results for classical spins and Carboni and Richards's infinite-temperature calculation for a linear chain of  $S = \frac{1}{2}$  quantum spins, there also exists an important model calculation which gives considerable insight into the time dependence of the spin-correlation functions. The appropriate model is called an  $XY$  model.<sup>8</sup> In this model, no exchange coupling exists between, say, the  $z$  components of the spins while the  $x$  and the  $y$  components are assumed to be bilinearly coupled among themselves by pairwise exchange potentials. It turns out that, for the particular case of  $S = \frac{1}{2}$  in one dimension, the mathematics relating to such a system of  $x$ - $x$  and  $y$ - $y$  coupled spins is exactly

\* Work forms part of a dissertation submitted to the Temple University in partial fulfillment of the requirements of the Ph.D. degree.

† Supported by an National Science Foundation predoctoral fellowship.

‡ Supported by the U. S. Office of Naval Research.

<sup>1</sup> See, for example, H. E. Stanley, in *Proceedings of the Ninth Latin American School of Physics*, edited by I. Saavedra (W. A. Benjamin, Inc., New York, 1968), Chap. 14, p. 833.

<sup>2</sup> R. Kubo and K. Tomita, *J. Phys. Soc. Japan* **9**, 888 (1954).

<sup>3</sup> C. G. Windsor, *Proc. Phys. Soc. (London)* **91**, 353 (1967); in *Neutron Inelastic Scattering* (International Atomic Energy Agency, Vienna, 1968), Vol. 2, p. 83.

<sup>4</sup> F. Carboni and P. M. Richards, *J. Appl. Phys.* **39**, 967 (1968); *Phys. Rev.* **177**, 889 (1969).

<sup>5</sup> M. Blume (private communication).

<sup>6</sup> G. H. Vineyard, R. E. Watson, and M. Blume, *J. Appl. Phys.* **39**, 969 (1968).

<sup>7</sup> R. E. Watson, M. Blume, and G. H. Vineyard, *Phys. Rev.* **181**, 811 (1969).

<sup>8</sup> E. Lieb, T. Schultz, and D. Mattis, *Ann. Phys. (N. Y.)* **16**, 407 (1961); S. Katsura, *Phys. Rev.* **127**, 1508 (1962); S. Katsura and S. Inawashiro, *J. Math. Phys.* **5**, 1091 (1964); M. Suzuki, *J. Phys. Soc. Japan* **21**, 2140 (1966).

reducible to that of a system of noninteracting fermions, as long as the range of the exchange interaction is restricted to the nn distance. In this manner, the dynamics of such an  $XY$  model has been exactly solved.<sup>9,10</sup>

In spite of the fact that the aforementioned exact calculations are undeniably valuable (i.e., in providing insights into the structure of the time-dependent properties of exchange-coupled spin system), their applicability is somewhat limited. For quantum spins, the Carboni-Richards<sup>4</sup> calculation as well as the  $XY$ -model results<sup>9,10</sup> are restricted to the case of one-dimensional spin- $\frac{1}{2}$  systems with only nn interactions. Similarly, the computer experiment calculations are feasible only for classical spins.

In our previous work,<sup>11</sup> we noted that a fairly adequate description of the time dependence in isotropic Heisenberg spin systems of arbitrary spin  $S$  and nn exchange interaction could be given via a phenomenological approximation for the frequency-wave-vector-dependent diffusivity. Bennett and Martin<sup>12</sup> first suggested that a possible sufficient approximation for the generalized diffusivity could be a two-parameter Gaussian. The spectral function, so constructed, then has a Lorentzian behavior in the limit of small frequencies and wave vectors (such a Lorentzian behavior is suggested by the phenomenological concept of local magnetization density), and also has finite frequency moments. This two-parameter approximation made use of the knowledge of the first three nontrivial frequency moments of the spectral function for the relevant spin-correlation function. [For isotropic paramagnets, in the absence of applied field, there is only one such spin-correlation function:  $\langle S_a^z(t)S_b^z(t') \rangle$ .] The results of our phenomenological theory made reasonable contact with the known results of the appropriate limiting cases, i.e., Carboni and Richards's exact calculation for one-dimensional array of  $S=\frac{1}{2}$  spins as well as the exact classical spin results of Ref. 3 for which we took the limit  $S \rightarrow \infty$ .

In our opinion, the usefulness of such a phenomenological theory lies in its great simplicity as well as its ability to give meaningful, if approximate, results for those intermediate cases for which the exact calculations are far too cumbersome to perform.

Continuing this general program, in the present paper, we study the time dependence of *anisotropic* Heisenberg spin systems where the Hamiltonian is of the form

$$\mathcal{H} = - \sum_{\sigma, p} [I_0(gp)S_\sigma^z S_p^z + I_+(gp)(S_\sigma^x S_p^x + S_\sigma^y S_p^y)]. \quad (1.1)$$

We assume that the exchange integrals  $I_0(gp)$  and

$I_+(gp)$  depend only upon the spatial separation of the positions labeled  $g$  and  $p$ , and that

$$I_0(gg) = I_+(gg) = 0. \quad (1.2)$$

As before, we again consider the system to be at an elevated temperature. However, unlike in Ref. 11, the range of the exchange interactions is now allowed to extend *beyond the nn distance*. Moreover, the integrals  $I_0$  and  $I_+$  are now, in general, allowed to be different. In the limit when  $I_+$  is vanishing, such a system reduces to a nondynamical Ising model, whereas the opposite limiting case of  $I_0=0$  corresponds to the  $XY$  model.

For the exactly soluble  $XY$  model<sup>9,10</sup> (a one-dimensional system of  $S=\frac{1}{2}$  spins with only nn  $I_+$  exchange), the results of our approximate theory are subjected to a searching scrutiny. We calculate the time dependence of the self-correlation  $\langle S_\sigma^z(t)S_\sigma^z(0) \rangle$  and the nn correlation  $\langle S_\sigma^z(t)S_1^z(0) \rangle$ . We examine the structure of the frequency Fourier transform  $\langle S_\sigma^z(t)S_\sigma^z(0) \rangle_\omega$  and we compute the frequency-wave-dependent longitudinal spectral function,  $F^{zz}(\mathbf{K}, \omega)$ , for various values of  $\mathbf{K}$ . These results are then compared with the exact ones computed from the appropriate expressions given in Refs. 9 and 10. The qualitative agreement of our approximate results with the exact ones is good. Moreover, the quantitative agreement is also, in general, satisfactory. However, we do find that within our phenomenological theory, the very sharp features of the exact results are often approximated with considerable rounding off at the edges.

In Sec. II, we first briefly outline the mathematical formalism of the dynamical spectral functions. Then we give the final results of the wave-vector-dependent frequency moments  $\langle \omega^n \rangle_{\mathbf{K}}^{\alpha\alpha}$ ,  $n=0, 1, 2$ , for the longitudinal and the transverse spectral functions valid for all spins  $S$ , arbitrary range of exchange interaction, and arbitrary dimensionality.

In Sec. III, an outline of the generalized diffusivity formulation is given, and the phenomenological approximation to be used is introduced.

Sections IV, V, and VI contain discussion of the frequency-wave-vector-dependent correlation functions for one-, two-, and three-dimensional systems, respectively.

The salient results of the paper are briefly recapitulated in the concluding Sec. VII.

## II. SPECTRAL FUNCTIONS

Unlike in Ref. 11, where in the paramagnetic regime we had only one type of spin-correlation function, in the present case there are a minimum of two different space-time-dependent spin-correlation functions

$$\langle [S_\sigma^\alpha(t), S_p^\alpha(t')]_+ \rangle \equiv F^{\alpha\alpha}(g-p, t-t'), \quad (2.1)$$

where  $\alpha=x, y, z$ . Because of assumed cylindrical symmetry, the correlations for  $\alpha=x$  and  $\alpha=y$  are identical. For convenience, we shall call these correlations the

<sup>9</sup> Th. Niemeijer, *Physica* **36**, 377 (1967); **39**, 313 (1968).

<sup>10</sup> S. Katsura, T. Horiguchi, and M. Suzuki, *Physica* (to be published).

<sup>11</sup> R. A. Tahir-Kheli and D. G. McFadden, *Phys. Rev.* **178**, 800 (1969); **182**, 604 (1969).

<sup>12</sup> H. S. Bennett and P. C. Martin, *Phys. Rev.* **138**, A608 (1965).

transverse correlations. The correlation with  $\alpha=z$  will, in general, be different from the transverse correlation and for convenience it will be called the longitudinal correlation function.

The dependence of these correlations upon the vector spatial separation  $(\mathbf{g}-\mathbf{p})$  and the time difference  $(t-t')$  is dictated by the appropriate translational invariance of the system Hamiltonian  $\mathcal{H}$ . This fact is most conveniently incorporated by using a Fourier representation

$$F^{\alpha\alpha}(\mathbf{g}-\mathbf{p}, t-t') = \frac{1}{N} \sum_{\mathbf{K}} e^{i\mathbf{K}\cdot(\mathbf{g}-\mathbf{p})} \times \int_{-\infty}^{+\infty} F^{\alpha\alpha}(\mathbf{K}, \omega) e^{-i\omega(t-t')} d\omega. \quad (2.2)$$

The sum is over a total of  $N$  allowed  $\mathbf{K}$  vectors which fall within the first Brillouin zone. When  $N$  is macroscopically large, i.e.,  $N \gg 1$ , the sum can as usual be replaced by an appropriate integral.

In Eq. (2.1), the pointed brackets designate a statistical average over a canonical ensemble, the notation  $[A, B]_{\pm}$  stands for  $AB+BA$ , and the time dependence of the spin operators is in the Heisenberg representation with respect to the Hamiltonian given in Eq. (1.1).

It is convenient to record the relevant symmetry properties of the spectral function  $F^{\alpha\alpha}(\mathbf{K}, \omega)$ . From the definition of  $F^{\alpha\alpha}(\mathbf{g}-\mathbf{p}, t-t')$  given in Eq. (2.1), we have

$$F^{\alpha\alpha}(\mathbf{g}-\mathbf{p}, t-t') = F^{\alpha\alpha}(\mathbf{p}-\mathbf{g}, t'-t). \quad (2.3)$$

Therefore, using Eq. (2.2), we get

$$F^{\alpha\alpha}(\mathbf{K}, \omega) = F^{\alpha\alpha}(-\mathbf{K}, -\omega). \quad (2.4a)$$

Because the system under consideration is invariant with respect to spatial inversions [see Eqs. (1.1) and (1.2)], therefore, we also have

$$F^{\alpha\alpha}(-\mathbf{K}, -\omega) = F^{\alpha\alpha}(\mathbf{K}, \omega). \quad (2.4b)$$

The spectral function is, therefore, even both in the inverse lattice vector  $K$  and in the frequency  $\omega$ .

The anticommutator correlation function  $F^{\alpha\alpha}(\mathbf{g}-\mathbf{p}, t-t')$  is closely related to the statistical correlation function  $\Phi^{\alpha\alpha}(\mathbf{g}-\mathbf{p}, t-t')$ ,

$$\Phi^{\alpha\alpha}(\mathbf{g}-\mathbf{p}, t-t') = \langle S_{\mathbf{g}}^{\alpha}(t) S_{\mathbf{p}}^{\alpha}(t') \rangle. \quad (2.5)$$

The relevant connection is established via the well-known machinery of the fluctuation-dissipation theorem. For present purposes, it suffices to give the relationship

$$\Phi^{\alpha\alpha}(\mathbf{g}-\mathbf{p}, t-t') = \int_{-\infty}^{+\infty} d\omega e^{-i\omega(t-t')} \times \langle S_{\mathbf{g}}^{\alpha}(t) S_{\mathbf{p}}^{\alpha}(t') \rangle_{\omega}, \quad (2.6a)$$

where

$$\langle S_{\mathbf{g}}^{\alpha}(t) S_{\mathbf{p}}^{\alpha}(t') \rangle_{\omega} = \frac{1}{N} \sum_{\mathbf{K}} e^{i\mathbf{K}\cdot(\mathbf{g}-\mathbf{p})} \frac{F^{\alpha\alpha}(\mathbf{K}, \omega)}{1+e^{-\beta\omega}}. \quad (2.6b)$$

The frequency moments of the spectral function  $F^{\alpha\alpha}(\mathbf{K}, \omega)$  are determined by time-independent statistical averages. To see how this comes about, let us find time derivatives of  $F^{\alpha\alpha}(\mathbf{g}-\mathbf{p}, t-t')$ , proceed to the limit  $t=t'$ , and sum over various position vectors in the following fashion:

$$\sum_{(\mathbf{g}-\mathbf{p})} e^{-i\mathbf{K}\cdot(\mathbf{g}-\mathbf{p})} \left[ \left( \frac{d}{dt} \right)^r \left( -\frac{d}{dt'} \right)^{n-r} F^{\alpha\alpha}(\mathbf{g}-\mathbf{p}, t-t') \right]_{t=t'} = \int_{-\infty}^{+\infty} F^{\alpha\alpha}(\mathbf{K}, \omega) \omega^n d\omega = \langle \omega^n \rangle_{\mathbf{K}}^{\alpha\alpha}. \quad (2.7)$$

Here, the sum is over all the position vectors  $(\mathbf{g}-\mathbf{p})$ , including the origin. The variables  $n$  and  $t$  are positive integers or zero with the condition that  $n \geq r$ .

In the limit of infinite temperature, Eq. (2.6b) becomes

$$\lim_{\beta \rightarrow 0} \langle S_{\mathbf{g}}^{\alpha}(t) S_{\mathbf{p}}^{\alpha}(t') \rangle_{\omega} = \frac{1}{2N} \sum_{\mathbf{K}} e^{i\mathbf{K}\cdot(\mathbf{g}-\mathbf{p})} F^{\alpha\alpha}(\mathbf{K}, \omega). \quad (2.8a)$$

Therefore, an alternative way of calculating the moments for infinite temperature is

$$\lim_{\beta \rightarrow 0} \langle \omega^n \rangle_{\mathbf{K}}^{\alpha\alpha} = 2 \sum_{(\mathbf{g}-\mathbf{p})} e^{-i\mathbf{K}\cdot(\mathbf{g}-\mathbf{p})} \times \left[ \left( \frac{d}{dt} \right)^r \left( -\frac{d}{dt'} \right)^{n-r} \Phi^{\alpha\alpha}(\mathbf{g}-\mathbf{p}, t-t') \right]_{t=t'}, \quad (2.8b)$$

where  $n \geq r$  and both  $n$  and  $r$  can take on positive integral values, including zero.

Because of the evenness of the spectral function  $F^{\alpha\alpha}(\mathbf{K}, \omega)$  in  $\omega$ , all odd frequency moments, i.e.,  $\langle \omega^{2n+1} \rangle_{\mathbf{K}}^{\alpha\alpha}$ , are identically vanishing. In the literature,<sup>13</sup> the first three even moments  $\langle \omega^{2n} \rangle_{\mathbf{K}}^{\alpha\alpha}$ ,  $n=0, 1$ , and  $2$ , have been calculated for the special case of isotropic exchange interactions in the limit of infinite temperatures. (After the present paper was completed, we came across a recent calculation of Huber and Semura,<sup>14</sup> who have given  $\langle \omega^{2n} \rangle_{\mathbf{K}}^{\alpha\alpha}$ , for  $n=0, 1, 2$  at infinite temperatures, for the special case of one-dimensional  $S=\frac{1}{2}$  spins with nn anisotropic exchange interactions.)

The procedure for computation of the moments  $\langle \omega^{2n} \rangle_{\mathbf{K}}^{\alpha\alpha}$  for  $n \geq 1$  is to make use of either of the two expressions (2.7) or (2.8b). The time derivatives are found as usual by making a repeated application of the quantum-mechanical rule

$$\frac{d}{dt} S_{\mathbf{g}}^{\alpha}(t) = [S_{\mathbf{g}}^{\alpha}(t), \mathcal{H}]_{-}. \quad (2.9)$$

The resultant time-independent statistical averages, of the form  $\langle A_{\mathbf{g}} B_{\mathbf{p}} \rangle$ , are computed by employing the well-

<sup>13</sup> M. F. Collins and W. Marshall, Proc. Phys. Soc. (London) **92**, 390 (1967); W. Marshall, in *Critical Phenomena*, edited by M. S. Green and J. V. Sengers (National Bureau of Standards, Washington, D. C., 1966), Vol. 273.

<sup>14</sup> D. L. Huber and J. S. Semura, Phys. Rev. **182**, 602 (1969).

known high-temperature expansion procedure

$$\begin{aligned} \langle A_g B_p \rangle &= \frac{\text{Tr}(e^{-\beta \mathcal{H}} A_g B_p)}{\text{Tr}(e^{-\beta \mathcal{H}})} \\ &= \frac{\text{Tr}[(1 - \beta \mathcal{H} + \beta^2 \mathcal{H}^2 / 2! - \dots)(A_g B_p)]}{\text{Tr}(1 - \beta \mathcal{H} + \beta^2 \mathcal{H}^2 / 2! - \dots)}. \end{aligned} \quad (2.10)$$

Because of the fact that in the present paper we are interested only in the dominant  $\beta$  dependence, the terms proportional to higher powers of  $\beta$  are ignored.

The zeroth moment follows easily from Eq. (2.8b),

$$\langle \omega^0 \rangle_{\mathbf{K}}^{\alpha\alpha} = 2 \sum_{(g-p)} e^{-i\mathbf{K} \cdot (\mathbf{g}-\mathbf{p})} \frac{\text{Tr}(S_g^\alpha S_p^\alpha)}{\text{Tr}(1)} = 2X, \quad (2.11)$$

where

$$X = \frac{1}{2} S(S+1). \quad (2.12)$$

Thus, at infinite temperatures, the zeroth moment has no  $\mathbf{K}$  dependence and is the same for all lattice structures.

The computation of the moments  $\langle \omega^{2n} \rangle_{\mathbf{K}}^{\alpha\alpha}$  is similarly simple for  $n=1$ . For  $n=2$ , the details are tedious, although still quite straightforward. In the following, we shall only record the final results. These results are valid for general spin and lattice dimensionality, arbitrary range of the exchange interaction  $I(gp)$ , and infinite temperatures.

$$\langle \omega^2 \rangle_{\mathbf{K}}^{zz} = 16X^2 \sum_{\mathbf{R}} (1 - e^{i\mathbf{K} \cdot \mathbf{R}}) I_+^2(\mathbf{R}), \quad (2.13a)$$

$$\begin{aligned} \frac{\langle \omega^4 \rangle_{\mathbf{K}}^{zz}}{64X^3} &= \frac{1}{5} \sum_{\mathbf{R}} (e^{i\mathbf{K} \cdot \mathbf{R}} - 1) I_+^2(\mathbf{R}) \left[ \left( 4 + \frac{3}{2X} \right) I_0^2(\mathbf{R}) + \left( 16 + \frac{1}{X} \right) I_+^2(\mathbf{R}) \right] + \sum_{\mathbf{R}} \sum_{\mathbf{A}} \{ 4e^{i\mathbf{K} \cdot \mathbf{R}} I_+(\mathbf{R}+\mathbf{A}) I_+(\mathbf{R}) I_+(\mathbf{A}) \\ &\times [I_0(\mathbf{A}) - I_0(\mathbf{R})] + 2(1 - e^{i\mathbf{K} \cdot \mathbf{R}}) I_+^2(\mathbf{R}) I_0(\mathbf{A}) [I_0(\mathbf{A}) - I_0(\mathbf{R}+\mathbf{A})] \\ &+ (1 - e^{i\mathbf{K} \cdot \mathbf{R}}) I_+^2(\mathbf{R}) (5 - 3e^{i\mathbf{K} \cdot \mathbf{A}}) I_+^2(\mathbf{A}) \}; \end{aligned} \quad (2.13b)$$

$$\langle \omega^2 \rangle_{\mathbf{K}}^{xx} = 8X^2 \sum_{\mathbf{R}} [I_+^2(\mathbf{R}) + I_0^2(\mathbf{R}) - 2e^{i\mathbf{K} \cdot \mathbf{R}} I_+(\mathbf{R}) I_0(\mathbf{R})], \quad (2.14a)$$

$$\begin{aligned} \frac{\langle \omega^4 \rangle_{\mathbf{K}}^{xx}}{64X^3} &= \sum_{\mathbf{R}} \left[ -\frac{1}{5} \left( \frac{1}{2X} + 3 \right) I_0^4(\mathbf{R}) + \frac{1}{5} \left( \frac{1}{2X} + 8 \right) e^{i\mathbf{K} \cdot \mathbf{R}} I_+(\mathbf{R}) I_0^3(\mathbf{R}) - \frac{3}{5} \left( \frac{1}{4X} + 4 \right) [I_+(\mathbf{R}) I_0(\mathbf{R})]^2 \right. \\ &+ \frac{2}{5} \left( \frac{1}{X} + 6 \right) e^{i\mathbf{K} \cdot \mathbf{R}} I_+^3(\mathbf{R}) I_0(\mathbf{R}) - \left. \left( \frac{1}{4X} + 1 \right) I_+^4(\mathbf{R}) \right] + \sum_{\mathbf{R}} \sum_{\mathbf{A}} \{ \frac{3}{2} [I_0(\mathbf{R}) I_0(\mathbf{A})]^2 \\ &- 2e^{i\mathbf{K} \cdot \mathbf{R}} I_+(\mathbf{R}) I_0(\mathbf{A}) I_0(\mathbf{R}) [I_0(\mathbf{R}+\mathbf{A}) + 2I_0(\mathbf{A})] + e^{i\mathbf{K} \cdot \mathbf{R}} I_+(\mathbf{R}+\mathbf{A}) I_+(\mathbf{A}) I_0(\mathbf{A}) [3I_0(\mathbf{R}+\mathbf{A}) + 2I_0(\mathbf{R})] \\ &+ I_0^2(\mathbf{R}) [3I_+^2(\mathbf{A}) + e^{i\mathbf{K} \cdot \mathbf{R}} I_+(\mathbf{A}) I_+(\mathbf{R}+\mathbf{A})] - 2I_+(\mathbf{R}) I_+(\mathbf{A}) I_+(\mathbf{R}+\mathbf{A}) I_0(\mathbf{R}+\mathbf{A}) \\ &+ 2e^{i\mathbf{K} \cdot \mathbf{R}} I_+^2(\mathbf{A}) I_+(\mathbf{R}) [I_0(\mathbf{R}+\mathbf{A}) - 3I_0(\mathbf{R})] + \frac{5}{2} [I_+(\mathbf{R}) I_+(\mathbf{A})]^2 - e^{i\mathbf{K} \cdot \mathbf{R}} I_+^2(\mathbf{R}) I_+(\mathbf{A}) I_+(\mathbf{R}+\mathbf{A}) \}. \end{aligned} \quad (2.14b)$$

In the isotropic limit, i.e.,  $I_+(\mathbf{R}) = I_0(\mathbf{R})$ , the transverse and the longitudinal moments are the same and correspond to the calculations of Collins and Marshall.<sup>13</sup> Also contained within Eqs. (2.13a) and (2.13b) are the results of Huber and Semura<sup>14</sup> for the special case of a linear chain with anisotropic nn exchange and  $S = \frac{1}{2}$ . To the best of our knowledge, the transverse moments are entirely new.

Note that in the long-wavelength limit, i.e.,  $\mathbf{K} \ll 1$ , the longitudinal moments go to zero. This is not the case for the transverse moments except in the isotropic limit.

### III. FORMULATION

A few low-order frequency moments of the spectral function  $F^{\alpha\alpha}(\mathbf{K}, \omega)$  were calculated in Sec. III in the limit  $\beta \rightarrow 0$ . These moments by themselves provide only limited information about the time dependence of the correlation functions  $F^{\alpha\alpha}(g-p, t-t')$  and  $\Phi^{\alpha\alpha}(g-p,$

$t-t')$ . Indeed, since

$$\begin{aligned} F^{\alpha\alpha}(g-p, t-t') &= \frac{1}{N} \sum_{\mathbf{K}} e^{i\mathbf{K} \cdot (\mathbf{g}-\mathbf{p})} \\ &\times \sum_{n=0}^{\infty} \frac{\langle \omega^n \rangle_{\mathbf{K}}^{\alpha\alpha} [-i(t-t')]^n}{n!} \end{aligned} \quad (3.1a)$$

and

$$\begin{aligned} \lim_{\beta \rightarrow 0} \Phi^{\alpha\alpha}(g-p, t-t') &= \frac{1}{2N} \sum_{\mathbf{K}} e^{i\mathbf{K} \cdot (\mathbf{g}-\mathbf{p})} \\ &\times \sum_{n=0}^{\infty} \frac{\langle \omega^n \rangle_{\mathbf{K}}^{\alpha\alpha} [-i(t-t')]^n}{n!} \end{aligned} \quad (3.1b)$$

[compare Eqs. (2.2), (2.6a), and (2.6b)], it follows that the knowledge of the first few frequency moments only enables us to determine the short-time (difference) behavior of these correlation functions.

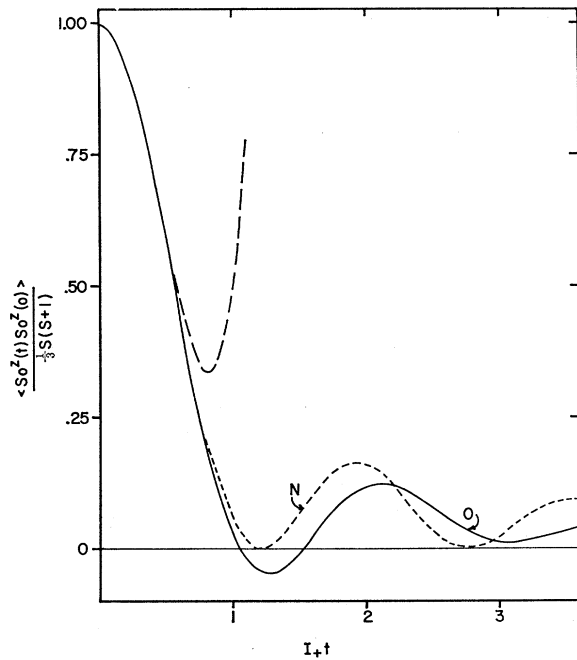


FIG. 1. Time dependence of the longitudinal self-correlation function for the restricted XY model. This model refers to a one-dimensional array of  $S=\frac{1}{2}$  spins coupled via nn exchange only, i.e.,  $I_0(R)=0$  for all  $R$  and  $I_+(R)=I_+$  for  $R=nn$  separation only. The solid curve marked O shows the results of the present phenomenological approximation, while the short dashed curve marked N is obtained by numerically computing the exact result given by Niemeijer [see Ref. 9, Eq. (23); compare also Ref. 10, Fig. 1]. The unmarked curve, with long dashes, is obtained by using the straightforward short time (i.e., the so-called moment) expansion up to and including the 4<sup>th</sup> term.

In practice, the knowledge of the short-time behavior of these correlation functions is of rather limited usefulness. For example, the understanding of the low-frequency phenomena, such as is recorded by the magnetic scattering of slow long-wavelength neutrons, the various electromagnetic field-resonance experiments performed in the laboratory, and the various transport phenomena are dependent upon the knowledge of the long-time behavior of these correlation functions.

If we think in terms of a particle analogy, the long-time description of an interacting many-particle system must take account of a situation which has, in general, entailed many interparticle collisions. [Note that, in the spin picture, a possible analog of such a collision is a mutual exchange of a single "spin flip." The terminology being used here is such that a spin of magnitude  $S$  can be flipped a total of  $(2S+1)$  times.] A well-known description of the collision-dominated behavior, which obtains in the limit of long wavelengths or equivalently small  $\mathbf{K}$  vectors, is in terms of hydrodynamics. In the study of the two-spin correlations  $\Phi^{\alpha\alpha}(g-p, t-t')$ , the appropriate hydrodynamic description to look for is that relating to the diffusion of magnetization density  $\langle S_\sigma^\alpha(t) \rangle_{(inequilibrium)}$ . Therefore, what is needed here is a formulation which makes use of the

rather meager information available about the system in the form of  $\langle \omega^{2n} \rangle_{\mathbf{K}}$ ,  $n=0, 1, 2$ , and which is powerful enough to provide insights into the appropriate hydrodynamics. As demonstrated in Ref. 11, the work of Martin and co-workers<sup>12,15</sup> provides just such a formulation. In this section, we shall only record the appropriate final results of this formulation which are of direct use in the following sections.

A useful spectral representation for the correlation functions  $F^{\alpha\alpha}(g-p, t-t')$  and  $\Phi^{\alpha\alpha}(g-p, t-t')$  is in terms of the frequency-wave-vector dependent diffusivity  $D^{\alpha\alpha}(\mathbf{K}, \omega)$ . Such a diffusivity is, of course, a function of the fundamental spectral function  $F^{\alpha\alpha}(\mathbf{K}, \omega)$ , which determines these correlation function through Eqs. (2.2) and (2.6). The most convenient choice for the diffusivity is that given by the following definition:

$$\int_{-\infty}^{+\infty} \frac{\omega F^{\alpha\alpha}(\mathbf{K}, \omega)}{Z - \omega} d\omega = A^{\alpha\alpha}(\mathbf{K}) \left[ \left( 1 - \frac{1}{\pi} \int_{-\infty}^{+\infty} \frac{D^{\alpha\alpha}(\mathbf{K}, \omega)}{Z^2 - \omega^2} d\omega \right)^{-1} - 1 \right], \quad (3.2)$$

where  $Z$  is complex,  $\text{Im}Z \neq 0$ , and  $A^{\alpha\alpha}(\mathbf{K})$  is independent of  $Z$ . Since all the odd moments of the spectral function  $F^{\alpha\alpha}(\mathbf{K}, \omega)$  are identically vanishing, therefore, the diffusivity  $D^{\alpha\alpha}(\mathbf{K}, \omega)$  is even in  $\omega$  and the given even dependence of the right-hand side of Eq. (3.2) upon  $Z$  is consistent. Moreover, the spatial inversion symmetry of the system [see Eq. (1.1)] ensures evenness in the  $\mathbf{K}$  variable.

Equation (3.2) specifies an exact relationship between the spectral function  $F^{\alpha\alpha}(\mathbf{K}, \omega)$  and the diffusivity

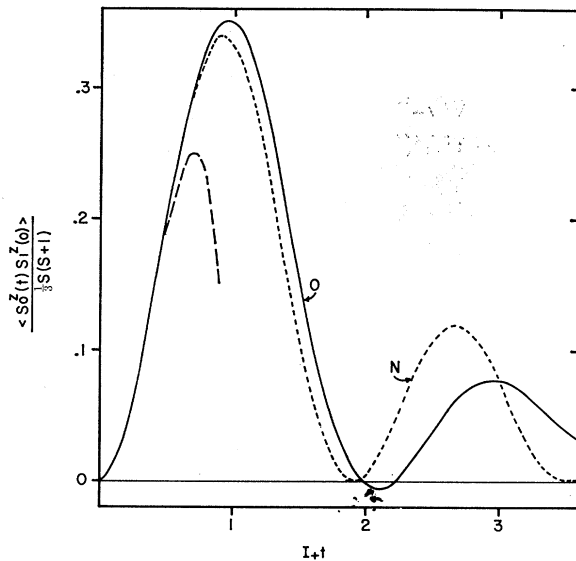


FIG. 2. This figure refers to the nn time-correlation function; otherwise, the explanation is similar to that given for Fig. 1.

<sup>15</sup> L. P. Kadanoff and P. C. Martin, Ann. Phys. (N. Y.) 24, 419 (1963).

$D^{\alpha\alpha}(\mathbf{K}, \omega)$ . The essential usefulness of this representation lies in the fact that, to an adequate accuracy, the diffusivity can be approximated by a simple Gaussian function

$$D^{\alpha\alpha}(\mathbf{K}, \omega) \sim \Delta^{\alpha\alpha}(\mathbf{K}) \Gamma^{\alpha\alpha}(\mathbf{K}) \exp\{-[\Gamma^{\alpha\alpha}(\mathbf{K})\omega]^2\}. \quad (3.3)$$

The three parameters  $A^{\alpha\alpha}(\mathbf{K})$ ,  $\Delta^{\alpha\alpha}(\mathbf{K})$ , and  $\Gamma^{\alpha\alpha}(\mathbf{K})$  are then exactly fixed by the relationships between the frequency moments  $\langle \omega^{2n} \rangle_{\mathbf{K}}$  with  $n=0, 1$ , and  $2$ , and  $\langle \Omega^{2n} \rangle_{\mathbf{K}}^{\alpha\alpha}$ :

$$\langle \Omega^{2n} \rangle_{\mathbf{K}}^{\alpha\alpha} = \frac{1}{\pi} \int_{-\infty}^{+\infty} D^{\alpha\alpha}(\mathbf{K}, \omega) \omega^{2n} d\omega, \quad (3.4)$$

with  $n=0$  and  $1$ . To derive these results we carry out small- $Z$  and large- $Z$  expansions, respectively, and compare coefficients. We get

$$A^{\alpha\alpha}(\mathbf{K}) = \langle \omega^0 \rangle_{\mathbf{K}}^{\alpha\alpha}, \quad (3.5a)$$

$$\langle \Omega^0 \rangle_{\mathbf{K}}^{\alpha\alpha} = \langle \omega^2 \rangle_{\mathbf{K}}^{\alpha\alpha} / \langle \omega^0 \rangle_{\mathbf{K}}^{\alpha\alpha}, \quad (3.5b)$$

$$\langle \Omega^2 \rangle_{\mathbf{K}}^{\alpha\alpha} + [\langle \Omega^0 \rangle_{\mathbf{K}}^{\alpha\alpha}]^2 = \langle \omega^4 \rangle_{\mathbf{K}}^{\alpha\alpha} / \langle \omega^0 \rangle_{\mathbf{K}}^{\alpha\alpha}. \quad (3.5c)$$

Equation (3.5a) specifies  $A^{\alpha\alpha}(\mathbf{K})$  and Eqs. (3.5b) and (3.5c) determine  $\Delta^{\alpha\alpha}(\mathbf{K})$  and  $\Gamma^{\alpha\alpha}(\mathbf{K})$ , i.e.,

$$\Delta^{\alpha\alpha}(\mathbf{K}) = \pi^{1/2} \langle \omega^2 \rangle_{\mathbf{K}}^{\alpha\alpha} / \langle \omega^0 \rangle_{\mathbf{K}}^{\alpha\alpha}, \quad (3.6a)$$

$$\Gamma^{\alpha\alpha}(\mathbf{K}) = \left( \frac{\langle \omega^0 \rangle_{\mathbf{K}}^{\alpha\alpha} \langle \omega^2 \rangle_{\mathbf{K}}^{\alpha\alpha}}{2[\langle \omega^0 \rangle_{\mathbf{K}}^{\alpha\alpha} \langle \omega^4 \rangle_{\mathbf{K}}^{\alpha\alpha} - (\langle \omega^2 \rangle_{\mathbf{K}}^{\alpha\alpha})^2]} \right)^{1/2}. \quad (3.6b)$$

Using Eqs. (3.2), (3.5a), (3.6a), and (3.6b), we find the final approximate expression for the spectral function  $F^{\alpha\alpha}(\mathbf{K}, \omega)$ , i.e.,

$$F^{\alpha\alpha}(\mathbf{K}, \omega) = \frac{\langle \omega^0 \rangle_{\mathbf{K}}^{\alpha\alpha} \Delta^{\alpha\alpha}(\mathbf{K}) \Gamma^{\alpha\alpha}(\mathbf{K}) \exp\{-[\omega \Gamma^{\alpha\alpha}(\mathbf{K})]^2\}}{\pi X^{\alpha\alpha}(\mathbf{K}, \omega)}, \quad (3.7a)$$

where

$$X^{\alpha\alpha}(\mathbf{K}, \omega) = \omega^2 \left( 1 - \frac{2\Delta^{\alpha\alpha}(\mathbf{K}) \Gamma^{\alpha\alpha}(\mathbf{K})}{\pi^{1/2} \omega} \right) \times \exp\{-[\omega \Gamma^{\alpha\alpha}(\mathbf{K})]^2\} \int_0^{\omega \Gamma^{\alpha\alpha}(\mathbf{K})} e^{x^2} dx \Big)^2 + (\Delta^{\alpha\alpha}(\mathbf{K}) \Gamma^{\alpha\alpha}(\mathbf{K}) \exp\{-[\omega \Gamma^{\alpha\alpha}(\mathbf{K})]^2\})^2. \quad (3.7b)$$

The expression above automatically conserves the frequency moments  $\langle \omega^n \rangle_{\mathbf{K}}$  for  $n=0, 1, \dots, 4$ . Moreover, in the hydrodynamic limit, it leads to the usual Lorentzian line shape for  $F^{\alpha\alpha}(\mathbf{K}, \omega)$ .

The adequacy of the phenomenological construct for the spectral line shape of  $F^{\alpha\alpha}(\mathbf{K}, \omega)$  given in Eqs. (3.7a) and (3.7b) has previously been demonstrated<sup>11</sup> for the isotropic Heisenberg paramagnet with only the nn interaction [compare also the following paper]. The present paper is concerned with investigation of the effects of exchange anisotropy as well as those occasioned by increasing the range of the exchange interactions.

#### IV. RESULTS IN ONE DIMENSION

The expressions for the frequency moments given in Eqs. (2.13) and (2.14) are valid for arbitrary range of the exchange integrals  $I_0(\mathbf{R})$  and  $I_+(\mathbf{R})$ , as well as for arbitrary lattice dimensionality. To study the case of a linear chain with nn and next-nearest-neighbor (nnn) exchange interactions only, it is greatly convenient first to recast these equations into the following particularized form:

$$\langle \omega^2 \rangle_{\mathbf{K}}^{zz} = 2[4XI_0(1)]^2 [(1-C_1)G^2 + (1-C_2)T_+^2], \quad (4.1a)$$

$$\begin{aligned} \langle \omega^4 \rangle_{\mathbf{K}}^{zz} / 256X^3 I_0^4(1) &= 2(C_2 - C_1)G^2 T_+(1 - T_0) + 2(C_1 - 1)G^2 T_0 + (C_2 - 1)T_+^2 + \frac{2}{5}[(C_1 - 1)G^2 + (C_2 - 1)(T_+ T_0)^2] \\ &+ 2[(1 - C_1)G^2 + (1 - C_2)T_+^2](1 + T_0^2) - (8/5)[(1 - C_1)G^4 + (1 - C_2)T_+^4] \\ &+ 5(G^2 + T_+^2)^2 + 3(C_1 G^2 + C_2 T_+^2)^2 - 8(C_1 G^2 + C_2 T_+^2)(G^2 + T_+^2) + (10X)^{-1} \\ &\times [(C_1 - 1)(G^4 + \frac{3}{2}G^2) + (C_2 - 1)(T_+^4 + \frac{3}{2}T_+^2 T_0^2)]; \end{aligned} \quad (4.1b)$$

$$\langle \omega^2 \rangle_{\mathbf{K}}^{xx} = 2[4XI_0(1)]^2 [-C_1 G - C_2 T_+ T_0 + \frac{1}{2}(G^2 + T_+^2 + 1 + T_0^2)], \quad (4.2a)$$

$$\begin{aligned} \langle \omega^4 \rangle_{\mathbf{K}}^{xx} / 256X^3 I_0^4(1) &= (1/20)(X^{-1} + 6)(-1 - T_0^4 + 4C_1 G^3 + 4C_2 T_+^3 T_0) \\ &+ (1/20)(X^{-1} + 16)(C_1 G + C_2 T_+ T_0^3 - \frac{3}{2}G^2 - \frac{3}{2}T_+^2 T_0^2) - \frac{1}{8}(X^{-1} + 4)(G^4 + T_+^4) \\ &+ \frac{3}{2}(1 + T_0^2)^2 + \frac{5}{2}(G^2 + T_+^2)^2 + 3(C_1 G + C_2 T_+ T_0)^2 - 4(C_1 + C_2 T_+ T_0)(1 + T_0^2) \\ &+ 3(G^2 + T_+^2)(1 + T_0^2) - G(C_1 G + C_2 T_+ T_0)(G^2 + T_+^2) + GT_+[C_1(-G^2 + 2 + T_+ + T_0) \\ &+ C_2(G - \frac{1}{2}GT_+) - GT_0 - 2G] + GT_0[C_1(G^2 - 2) + C_2(G + \frac{1}{2}T_0)] - C_2 T_+ T_0. \end{aligned} \quad (4.2b)$$

Here, for convenience we have introduced the abbreviation such that  $I_0(\mathbf{R})$  and  $I_+(\mathbf{R})$  denote the corresponding exchange integrals between the  $r$ th nn. Moreover,

$$\begin{aligned} G &\equiv I_+(1)/I_0(1), \quad T_+ \equiv I_+(2)/I_0(1), \\ T_0 &+ I_0(2)/I_0(1), \end{aligned} \quad (4.3a)$$

and

$$C_1 = \cos K, \quad C_2 = \cos 2K. \quad (4.3b)$$

The units have been chosen so that the nn separation is unity. Moreover, for convenience, exchange interactions between third and further neighbors have been assumed to be vanishing.

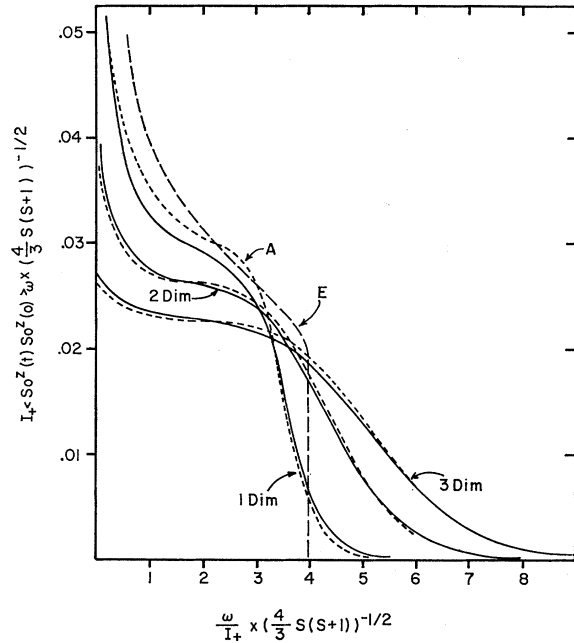


FIG. 3. Plot of the frequency Fourier transform of the longitudinal self-correlation function, as a function of the reduced frequency, for a generalized XY model with only nn exchange  $I_+$  and with arbitrary spin. The short dashed curves give our results for the case of spin  $\frac{1}{2}$ , whereas the full curve gives the corresponding results for spin  $\infty$ . The case of the restricted XY model, i.e., with  $S = \frac{1}{2}$  spins coupled via nn exchange only in one dimension, is exactly soluble. The corresponding exact results (computed from an expression derived by Katsura *et al.*) is given as a curve with long dashes and it is labeled E. This curve should be compared with the result of the present theory, which is marked A.

Some salient features of the above results for the frequency moments should be noted: In the long-wavelength limit, i.e.,  $K \ll 1$ , and for  $S > \frac{1}{2}$ , the longitudinal moments,  $\langle \omega^{2n} \rangle_{K^{zz}}$ ,  $n = 1, 2$ , go to 0 as  $(K)^2$  for all  $G$ ,  $T_0$ , and  $T_+$ . The case of spin  $\frac{1}{2}$ , however, is somewhat unique when  $T_+ = T_0 = 0$  and  $I_0(1)$  tends to 0. For this as  $K \rightarrow 0$ , the fourth frequency moment goes to 0 as  $(K)^4$ . As we shall see in the following, this feature has the consequence that for such an anisotropic limit the magnetization density for the case of  $S = \frac{1}{2}$  linear chain does not diffuse.

A. XY Limit

In one dimension, the limit  $I_0(R) = 0$  is particularly interesting. In this limit, the Hamiltonian (1.1) only contains the transverse spin components, i.e.,  $S^x$  and  $S^y$ . As is well known,<sup>8</sup> the mathematics of a system of XY spins of magnitude  $S = \frac{1}{2}$  with only the nn exchange coupling [to distinguish this special case from the more general case of arbitrary size spins and /or arbitrary range of exchange interaction  $I_+(\mathbf{R})$ , we shall call it the restricted XY model] can be made isomorphic with that of a system of noninteracting Fermi particles. This simplification enables one to obtain an exact solution of the physics of a restricted XY model.<sup>8-10</sup>

The availability of an exact solution of such an XY model is very fortunate because it provides a stringent test for the adequacy of the phenomenological theory proposed in Sec. III.

The predictions of the phenomenological theory regarding the time-dependent longitudinal correlations  $\langle S_0^z(t) S_0^z(0) \rangle$  and  $\langle S_0^z(t) S_1^z(0) \rangle$ , for the special case of a restricted XY model are plotted in Figs. 1 and 2, respectively. The corresponding computations are also carried out using the exact solution of Niemeijer<sup>9</sup> and for comparison are plotted in the same figures. The quantitative agreement is good for short times. However, for time  $t > (I_+)^{-1}$ , the agreement is seemingly only qualitative.

The relative usefulness of the phenomenological construct being employed here is well illustrated by a comparison with the corresponding results obtained by using a direct short-time expansion (this is the so-called moment expansion) given in Eq. (3.1b). Employing the known moments [this expansion is necessarily limited to the term  $(t)^4$  because we are not using higher-order (even) moments], the time dependence of the correlation functions is computed via Eq. (3.1b). These results are plotted as curves with long dashes, and their relative inadequacy, for times  $t > (2I_+)^{-1}$ , is clearly evident. Indeed, beyond these rather short times, the predictions of the straightforward moment expansion are totally unreasonable. In contrast, the present phenomenological theory (which uses the same basic information employed in the above moment expansion) gives quantitatively correct results for times which are twice as long. Sim-

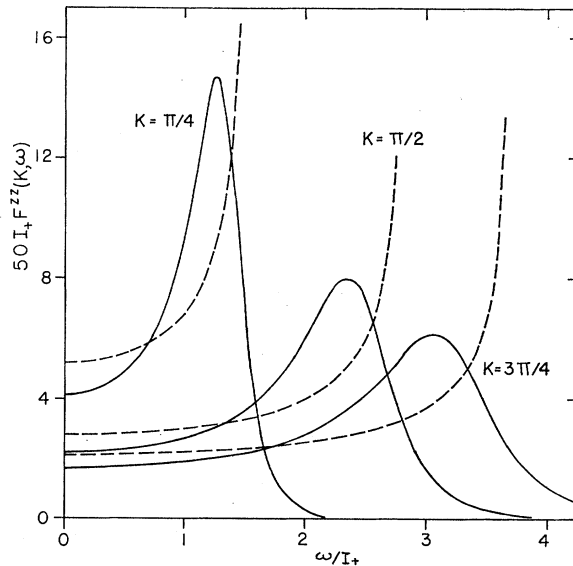


FIG. 4. For the restricted XY model, the results for the frequency-wave-vector Fourier transform of the longitudinal correlation function are displayed for  $K = n\pi/4$  with  $n = 1, 2$ , and 3. Note the extremely sharp divergence of the exact results (dashed curves) compared with the rounded-off maxima displayed by the corresponding approximate results given by the present theory (full curves). The exact results are computed from Eq. (55) of Ref. 10.

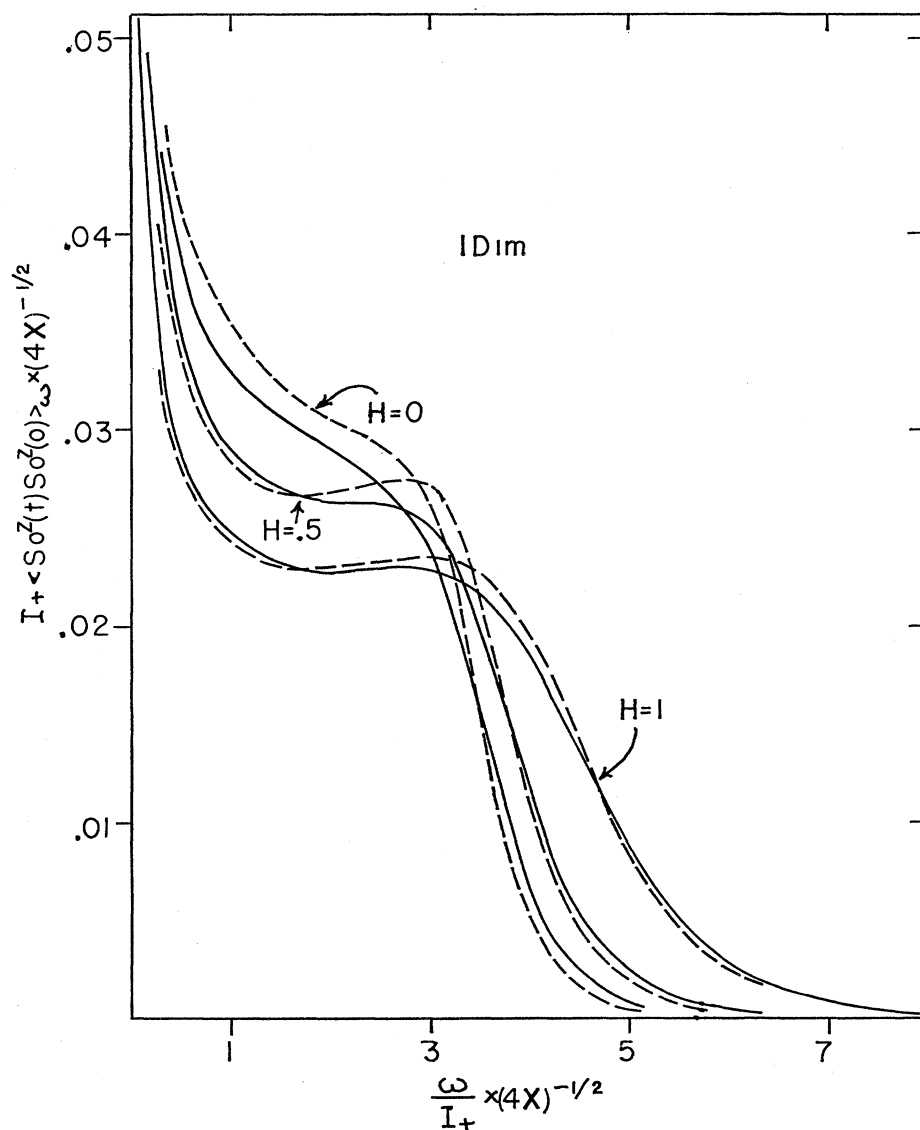


FIG. 5. Dependence of the frequency Fourier transform of the longitudinal self-correlation function for a one-dimensional generalized  $XY$  model. Here, the size of the second-neighbor exchange relative to the nn exchange is denoted by

$$H = I_+(2)/I_+(1)$$

and

$$X = S(S+1)/3.$$

The dashed curves are for spin  $\frac{1}{2}$  and the solid curves for spin  $\infty$ .

ilarly, as we shall see later in this section, the qualitative long-time behavior of the correlation functions is also correctly predicted by the present phenomenological theory. Moreover, in the intermediate-time regime, the results of the present theory are vaguely of the correct order of magnitude, whereas the moment expansion cannot make any such claims.

Let us next examine the hydrodynamic structure of the more general  $XY$  model. Since the restricted  $XY$  model referred to earlier can be reduced to a (hypothetical) system of noninteracting Fermi particles, and since noninteracting particles systems do not undergo collisions in the normal sense, it follows that the restricted  $XY$  model does not possess any hydrodynamics as such.<sup>16</sup> For this reason, we write the corresponding

<sup>16</sup> Compare with K. Kawasaki, Ann. Phys. (N. Y.) **37**, 142 (1966).

results for the low-frequency limit of the function  $D^{zz}(K, \omega)$ . [Note that because  $I_0(\mathbf{R})=0$ , for an  $XY$  model, therefore, some slight care must be exercised in converting the given frequency moments, i.e., as displayed in Eqs. (4.1a) and (4.1b), to an appropriate form valid for  $I_0(1) \rightarrow 0$ .] Making use of Eqs. (3.3), (3.6a), and (3.6b), we get the desired expression for nn exchange but arbitrary spin

$$D^{zz}(K, \omega) = 4I_+(1)(1-C_1) \times \left( \frac{\pi X}{7/5 - 1/10X - C_1} \right)^{1/2} \times \exp\left( \frac{-\omega^2}{16I_+^2(1)X(7/5 - 1/10X - C_1)} \right). \quad (4.4)$$

For  $S = \frac{1}{2}$ ,  $7/5 - 1/10X = 1$ . Therefore, except in the limit of the restricted  $XY$  model, the diffusivity is



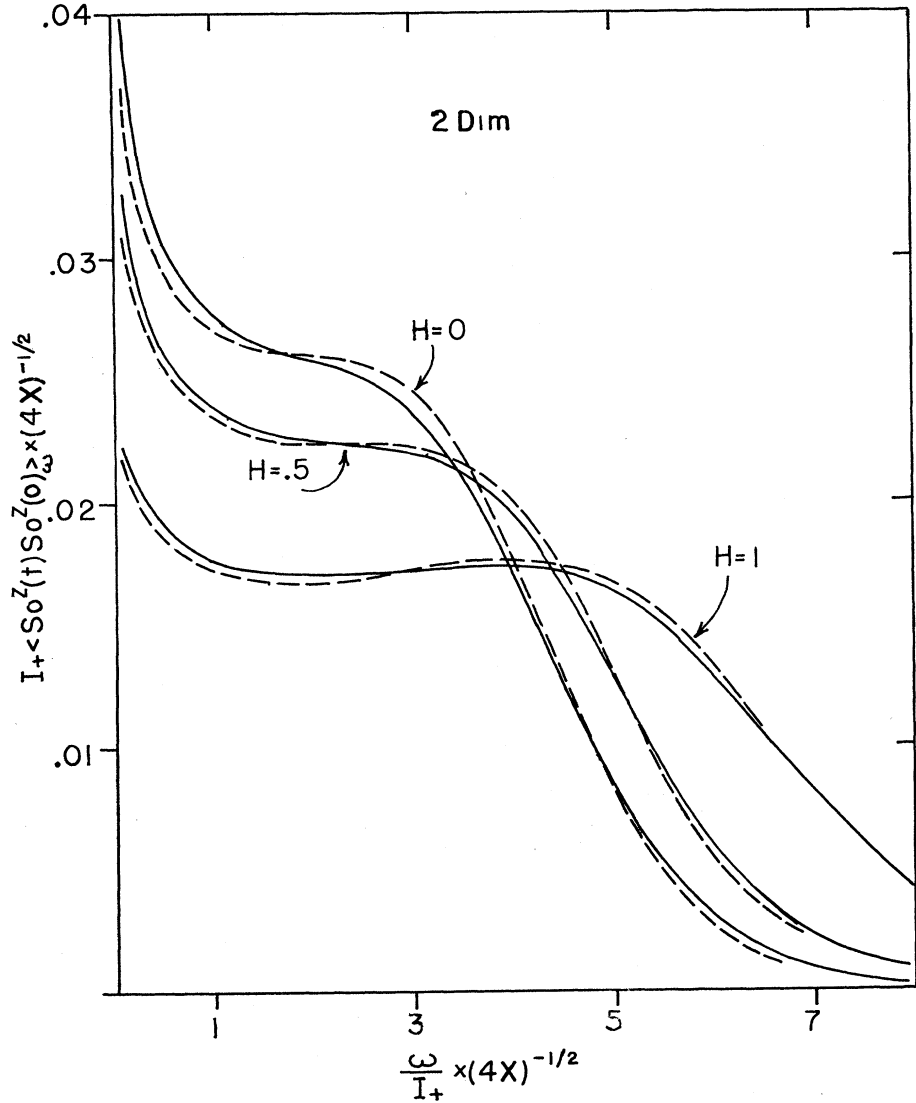


FIG. 6. As in Fig. 5, the dependence of the frequency Fourier transform for the longitudinal self-correlation upon the magnitude of the spin and the second-neighbor exchange is shown for a generalized XY model. These results, however, refer to a two-dimensional square lattice.

clearly seen to be hydrodynamic because for small  $K$  it shows a quadratic dependence upon  $K$ . For the restricted XY model, the diffusivity has a nonhydrodynamic linear dependence upon  $K$  as  $K \ll 1$ . This point will be elaborated further in the following.

To get a feel for the line shape of  $F^{zz}(K, \omega)$  for small  $\omega$ , let us use the expression for the diffusivity given in Eq. (4.4) in Eqs. (3.7a) and (3.7b). The appropriate result is of the form

$$F^{zz}(K, \omega)_{(\omega/I_+) \ll 1, K \ll 1} \sim \frac{aK^2}{b\omega^2 + cK^4}, \quad (4.5)$$

where  $a$ ,  $b$ , and  $c$  are independent of  $\omega$  and  $K$  (except for the case of the restricted XY model discussed below). Therefore, the frequency-dependent longitudinal-correlation functions are strongly divergent in the limit  $\omega \rightarrow 0$ .

For the restricted XY model, the variables  $a$  and  $c$  are, however, easily seen to be  $K$ -dependent and, in the limit  $K \ll 1$ , we have

$$a = a'(1/K), \quad c = c'(1/K)^2, \quad (4.6)$$

where  $a'$  and  $c'$  are independent of  $K$  and  $\omega$ . Therefore,

$$[F^{zz}(\mathbf{K}, \omega)]_{(\text{Restricted XY})} \underset{\omega/I_+ \ll 1, K \ll 1}{\sim} \frac{a'K}{b\omega^2 + c'K^2}. \quad (4.7)$$

The divergence of the frequency Fourier transforms of the longitudinal correlation is, therefore, somewhat weaker for the restricted XY model. Indeed, we may expect the divergence to be logarithmic according to the following simple argument. Insert Eq. (4.7) into Eq. (2.6b) and replace the sum by an integral. We

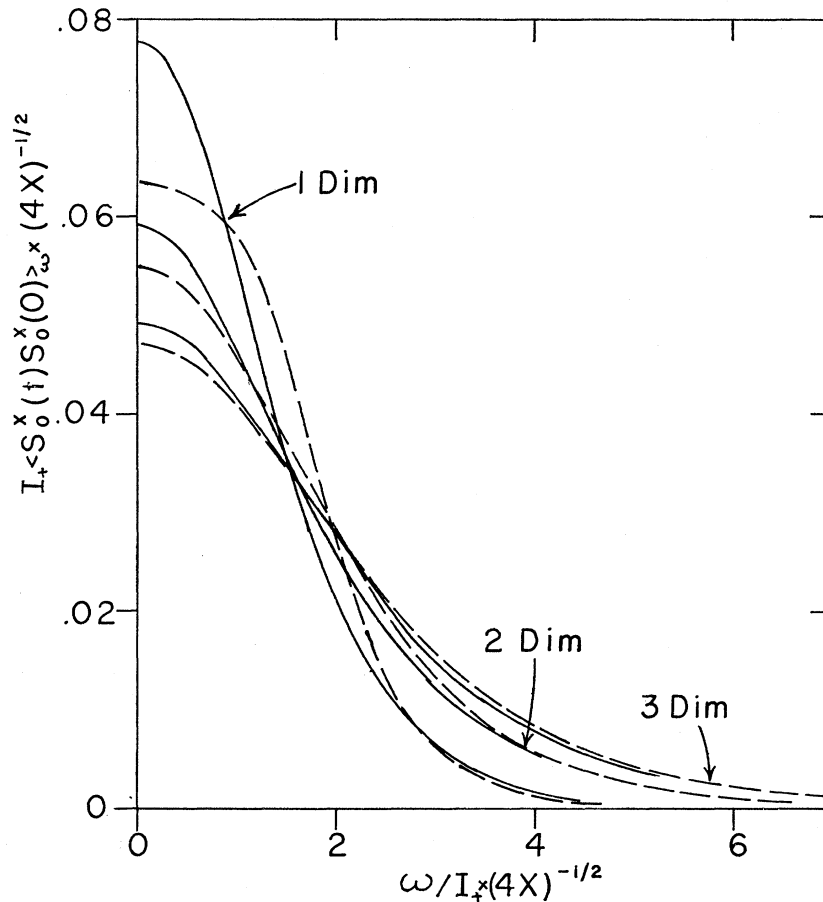


FIG. 7. Plot of frequency Fourier transforms of the transverse self-correlation function for the XY model with nn exchange and spins of magnitude  $S = \frac{1}{2}$  (dashed curves) and  $S = \infty$  (full curves). From a mutual comparison of the  $S = \frac{1}{2}$  and  $S = \infty$  curves, the validity of a law of corresponding states can be established, except in one dimension in the small frequency regime, i.e.,

$$(\omega/I_+) (4X/9)^{-1/2} < 0.5.$$

get

$$\lim_{\beta \rightarrow 0} [\langle S_{\theta}^z(t) S_{\rho}^z(0) \rangle_{\omega}] = \frac{1}{4\pi} \int_{-\pi}^{+\pi} dK \cos[K(g-p)] F^{zz}(K, \omega). \quad (4.8)$$

Note that the dominant contribution to the integral comes from small- $K$  values. For these small- $K$  values, the cosine may be replaced by unity. Therefore, the correlation  $\langle S_{\theta}^z(t) S_{\rho}^z(0) \rangle_{\omega}$  has a positive logarithmic divergence at the origin  $\omega = 0$ .

The logarithmic frequency dependence for small  $\omega$  suggests the following simple time-dependent behavior in the limit of long times:

$$\lim_{\beta \rightarrow 0, t \rightarrow \infty} [\langle S_{\theta}^z(t) S_{\rho}^z(0) \rangle]_{(\text{Restricted } XY)} \propto t^{-1}. \quad (4.9)$$

Such a slow time decay is in accord with the exact solution.

As mentioned earlier for the generalized XY model, where either the range of the exchange interaction is longer than nn distance, or where  $S > \frac{1}{2}$ , no exact solutions are available. Since one of the major advantages of the present phenomenological theory is that it allows

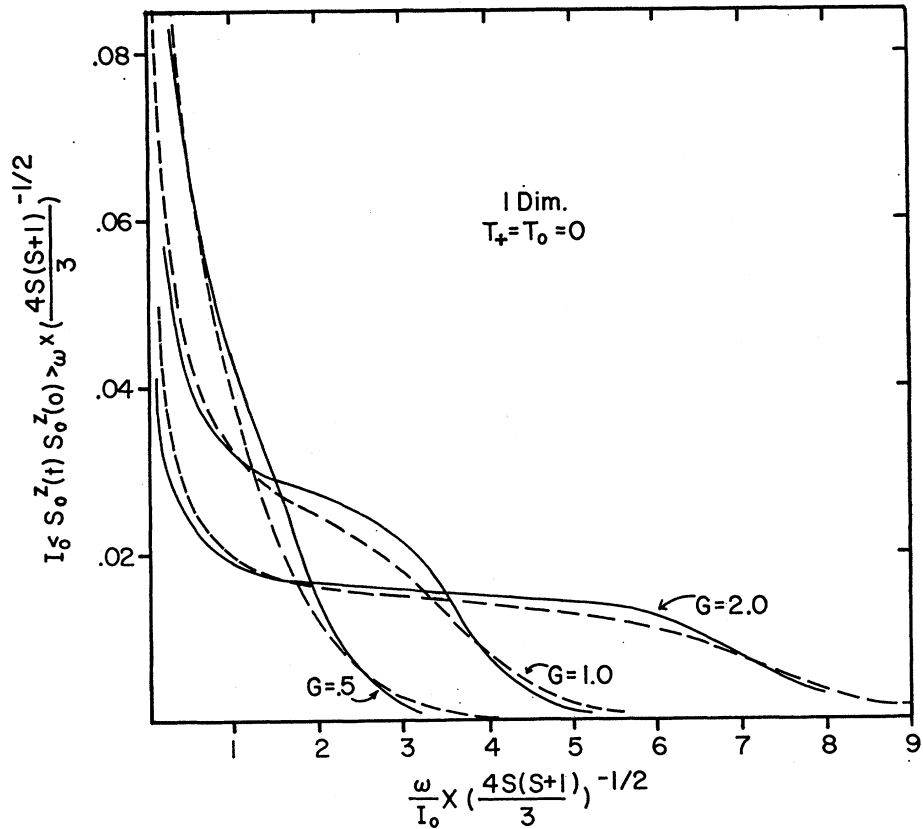
us to discuss the properties of these more general situations as easily as those for which exact *ab initio* solutions are available [compare Ref. 11], we have computed the dynamical structure of the correlation functions for this case also. The corresponding results for the longitudinal correlations are given in Figs. 3-5.

The exact results, given in Fig. 3, are obtained from an expression derived by Katsura *et al.* [see Ref. 10, Eq. (31)]. The predictions of our phenomenological theory, once again, seem to be qualitatively verified. Indeed, notwithstanding the slight rounding off of the phenomenological results as compared to the rather sharp cutoff shown by the exact result, even the quantitative predictions of our theory are not too inadequate.

From an examination of the results given in Figs. 3-5, the following general comments can be made:

(1) To a reasonable approximation, a law of corresponding states (discussed in Ref. 11) again holds. This law can be stated as follows: In terms of an appropriate reduced scale, i.e., when  $I_+ \langle S_{\theta}^z(t) S_{\rho}^z(0) \rangle_{\omega} \times (4X)^{-1/2}$  is plotted against  $(\omega/I_+) (4X)^{-1/2}$ , the curves for different spin magnitudes are nearly the same. The accuracy of this empirical law increases with the in-

FIG. 8. Plot showing the effect of anisotropy on frequency Fourier transform of the longitudinal self-correlation function for a linear chain with only nn interactions. Here,  $G$  indicates the ratio of the transverse and the longitudinal exchange integrals, i.e.,  $G=I_+(1)/I_0(1)$ . The solid and dashed curves represent the results for spin  $\frac{1}{2}$  and spin  $\infty$ , respectively.



crease in the dimensionality as well as the range of interaction.

(2) In a crude fashion, the general effect of the increase of the effective range of the exchange interaction is to increase the magnitude of the cutoff frequency. Moreover, seemingly, the larger the effective range of the exchange interaction, the better the agreement with a law of corresponding states. (Compare with Fig. 6 for two dimensions and note that the effects of the increase in dimensionality are qualitatively similar to that of increase in the range of the exchange interactions.)

In contrast to the longitudinal correlations discussed above, the dynamical structure of the transverse correlations is quite different. The main reason for this is that the decay of the transverse correlations with the passage of time is much faster. This is reflected in the behavior of the low-frequency Fourier transforms of these correlations and, accordingly, in the limit of zero frequency, the transforms remain finite. Figure 7 displays the Fourier transform of the self-correlation  $\langle S_0^x(t) S_0^x(0) \rangle_\omega$  for spin  $S=\frac{1}{2}$  and  $S=\infty$ . A mutual comparison of the corresponding curves for  $S=\frac{1}{2}$  and  $S=\infty$  demonstrates the approximate validity of the above-mentioned law of corresponding states for the transverse case also. In one dimension, this empirical law seems to be very poorly followed for small frequencies, i.e.,  $(\omega/I_+) (4X)^{-1/2} < 0.5$ . As far as the authors are aware,

no exact results corresponding to the restricted XY model [see the curve for one dimension in Fig. 7] are available in the literature for the case of transverse spin correlation.

### B. General Anisotropic Case

For a one-dimensional system with anisotropic nn and nnn exchange, the given form of the frequency moments, i.e., Eqs. (4.1)–(4.3), is quite suitable for carrying out numerical computations as long as  $I_0(1)$  is not vanishing. When  $I_0(1)$  is equal to zero, these expressions must first be multiplied through by  $I_0(1)$ . In the normal manner, from these moments we determine the parameters  $\Delta^{\alpha\alpha}(K)$  and  $\Gamma^{\alpha\alpha}(K)$ , which because of the phenomenological approximation discussed earlier, in turn, specify the spectral function  $\Gamma^{\alpha\alpha}(K, \omega)$  [see Eqs. (3.7a) and (3.7b)].

The spectral function and the various space-time-dependent correlation functions  $\Phi^{\alpha\alpha}(g-p, t-t')$  that it determines are, thus, given as function of the ratios  $G$ ,  $T_+$ , and  $T_0$ . The dependence upon the magnitude of the spin variable  $S$  is, of course, always assumed. The two remaining system variables, i.e., the interspin separation and an exchange integral, say,  $I_0(1)$ , do not give rise to any explicit dependence. Rather they merely determine the units in which the space and time separations are measured.

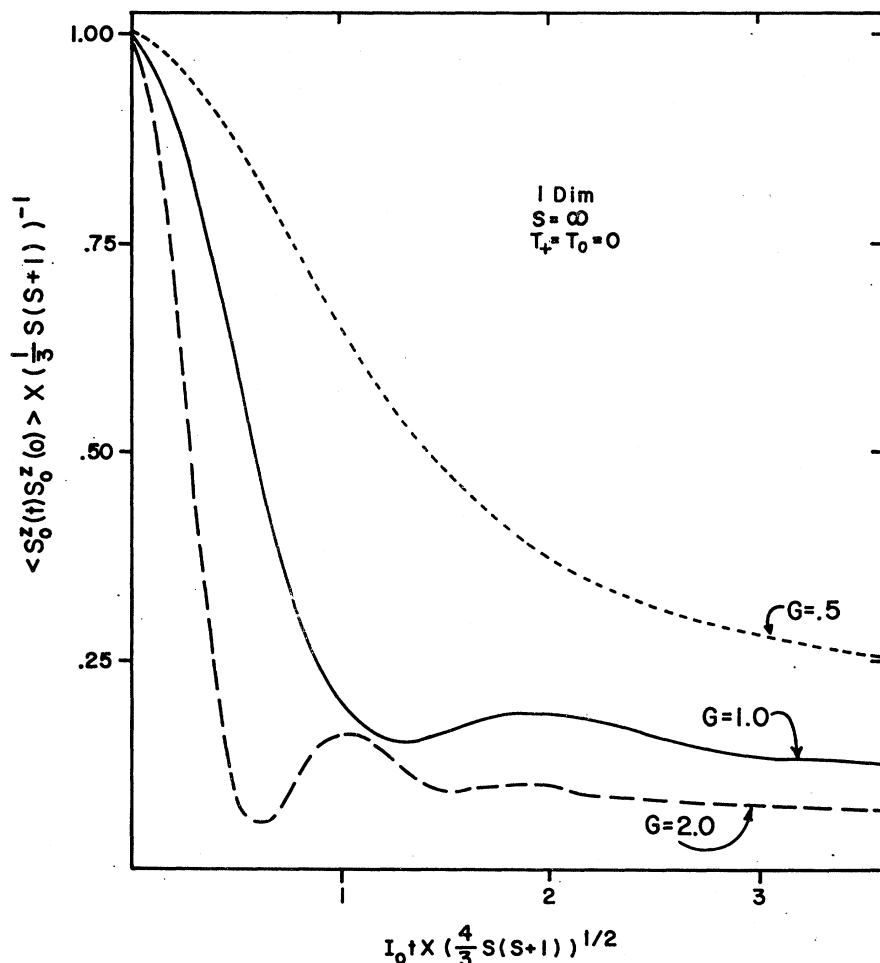


FIG. 9. Effect of anisotropy on the time dependence of the longitudinal self-correlation function for a linear chain with  $S = \infty$  and only nn interactions. This plot is an appropriate Fourier transform of the corresponding curves in Fig. 8. For  $G=0.5$ , the transverse exchange is only half as strong as the longitudinal exchange. Consequently, the time decay of the correlation is quite slow. (For the Ising model, i.e.,  $G=0$ , the curve would be a straight line with ordinate=1.) When  $G=2.0$ , the relative strength of the transverse exchange is greater and the system behaves somewhat similarly to an  $XY$  model (compare Fig. 1).

Let us first consider the case of nn interactions only. Here  $T_+ = T_0 = 0$  and the dynamical line shape is a function only of  $G$ . When  $G$  is large compared to unity, the system approaches the  $XY$  model studied above. For  $G \rightarrow 0$ , the system reduces to a nn Ising model.

In Fig. 8, we have displayed the results for the frequency Fourier transform of the longitudinal self-correlation function. As  $G$  is reduced from the isotropic limit, i.e.,  $G=1$ , the frequency spectrum is compressed towards lower frequencies. Indeed, the curves for  $G=1/2$  already seem to be anticipating the limiting results for the Ising model (which may be expected to have a strong  $\delta$  function at the origin). Similarly, the curves for  $G=2.0$  seem to be anticipating the results for the  $XY$  limit. Note, however, that the curves in Fig. 8 have been plotted on a different frequency scale from the corresponding results for the  $XY$  model given in Fig. 3. Here, the frequency is being measured in the units of  $\omega/I_0(1)$ . These units are, of course, not suitable for the  $XY$  model where  $I_0(\mathbf{R})=0$ .

These statements are further illustrated by looking at the time Fourier transforms as plotted in Fig. 9. For brevity, we give these results for spin  $\infty$  only. The

curve for  $G=2$  is clearly seen to be assuming the structure possessed by the  $XY$  model. [For example, compare with Fig. 1. The fact that Fig. 1 relates to  $S=1/2$  and the frequency scale there is in units of  $I_+$  does not affect the qualitative nature of the present argument.] In contrast, the curve for  $G=0.5$  clearly shows that the rate of decay with time of the correlation function has become much slower. In the true Ising limit, such a decay would completely cease because there the  $z$  component of each individual spin is a constant of motion (except, of course, for the infinitesimally slow time decay caused by thermal interactions with the heat bath which bring about thermodynamic equilibrium; here, we have neglected these small interactions).

The frequency Fourier transform of the nn longitudinal correlation is shown in Fig. 10. Here again, the above-mentioned trends are evident. Of course, here, in order to preserve the sum rule

$$\lim_{\beta \rightarrow 0} \int_{-\infty}^{+\infty} d\omega \langle S_0^z(t) S_n^z(0) \rangle_\omega = X \delta_{n,0}, \quad (4.10)$$

the spectrum must also dip below the frequency axis.

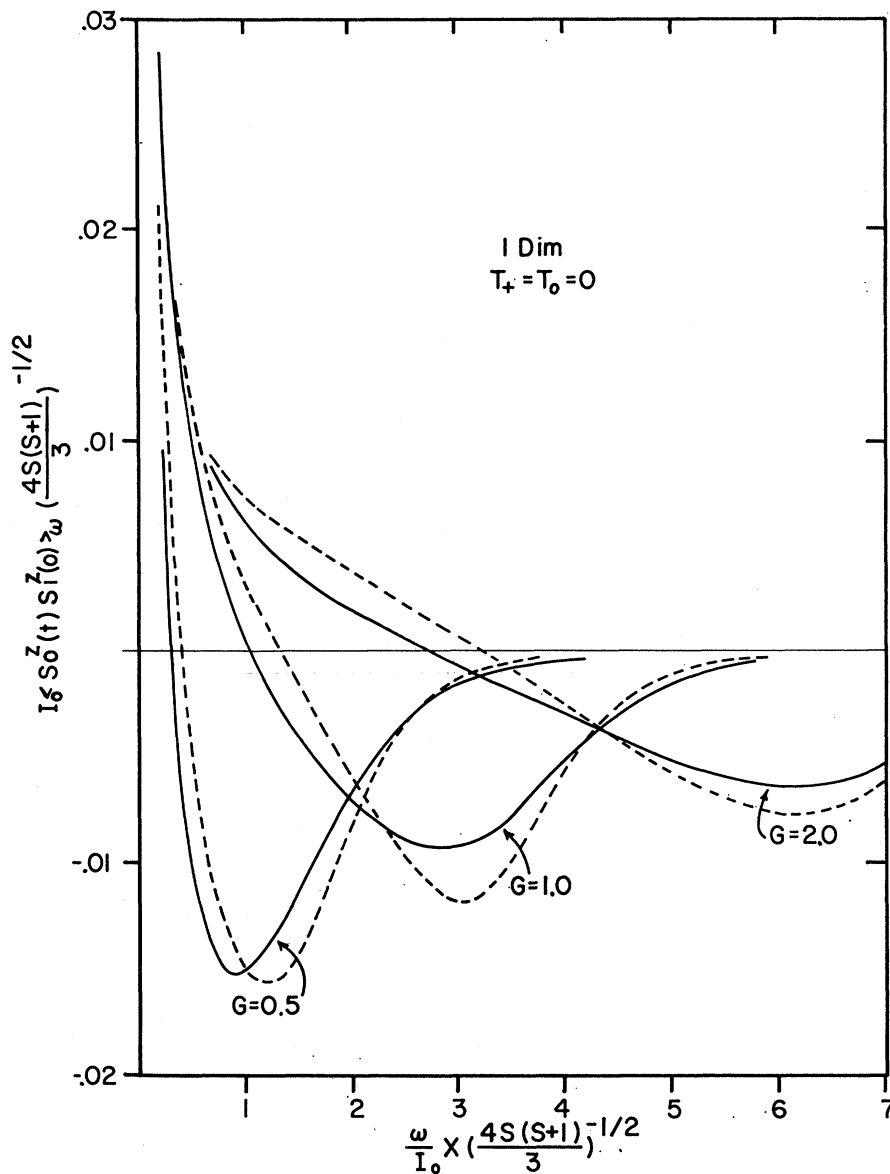


FIG. 10. Effect of anisotropy on frequency Fourier transform of the longitudinal nn correlation, plotted versus the reduced frequency, for the linear chain. The dashed and solid curves represent the results for spin  $\frac{1}{2}$  and spin  $\infty$ , respectively. As in Figs. 8 and 9, the ratio  $I_+(1)/I_0(1)$  is indicated by  $G$  and all further neighbor exchange is assumed to be vanishing.

Continuing the study of the nn anisotropic exchange case, we examine next the dynamical structure of the transverse self-correlation. In Fig. 11, the frequency Fourier transforms for the transverse self-correlation are plotted for various values of the anisotropy, i.e.,  $G=2, 1, 0.5$ , and for the case when  $S=\frac{1}{2}$  and  $\infty$ . When  $G=1$ , the results are, of course, identical to the corresponding results for the longitudinal self-correlation. For all other values of  $G$ , i.e.,  $G \neq 1$ , the small-frequency behavior of the transverse correlations differs dramatically from the corresponding longitudinal correlations in that it shows no divergence as  $\omega \rightarrow 0$ .

Heuristically, this behavior is easy to understand. The total  $z$  component of the spin is always a constant of motion. Therefore, under normal situations (i.e.,

excluding the anomalous behavior of the restricted XY model which is strictly nondiffusive), this gives rise to spin density diffusion, i.e., the local density of the  $z$  component of spins follows a diffusion equation in the long-wavelength long-time limit. The total  $x$  and  $y$  components of spin, on the other hand, are not constants of motion unless  $G=1$ . Therefore, the transverse components of spin density do not obey a diffusion equation.

It is instructive to compute the diffusion coefficient  $D^{zz}$  for the  $z$  component of the spin density, i.e.,

$$D^{zz} = \lim_{\omega \rightarrow 0, K \rightarrow 0} \left( \frac{D^{zz}(K, \omega)}{K^2} \right). \tag{4.11}$$

Within the present phenomenological approximation for nn exchange only, this yields

$$D^{zz} = 2I_0 G^2 \left( \frac{\pi X}{8/5 - 3/20X + G^2(2/5 - 1/10X)} \right)^{1/2}. \quad (4.12)$$

Let us next investigate the effects of increasing the range of the exchange interaction beyond the nn distance. Figures 12 and 13 illustrate some typical effects associated with such an increase in the range. These are (i) a gradual increase of the magnitude cutoff frequency and (ii) an improved agreement with the law of corresponding states referred to earlier.

In Fig. 14, we have displayed the time dependence of the self-correlation function for various (relative) sizes of the nnn exchange. For simplicity, the exchange has been assumed to be spatially isotropic. We find that with the increase in the relative magnitude of the nnn exchange, the initial rate of time decay becomes faster and consequently the relaxation time of the correlation

function decreases. This is quite in accord with a heuristic argument whereby the longer the range of interactions (and/or the larger the effective coordination number, i.e., the average number of spins which can be assumed to be interacting strongly with a given spin), the more accurately the behavior of the system may be expected to be approximated by nondynamical average field representations.

In other words, this means that for systems with many effective neighbors, the various occurrences are not expected to be too strongly correlated for long time intervals. It should also be mentioned here that a very reasonable agreement with the above picture also emerges when we study the effect of dimensionality on the structure of the time-dependent correlation [see Sec. VI and Fig. 23].

## V. RESULTS IN TWO DIMENSIONS

The relevant frequency moments, specialized to a quadratic lattice, with nn and nnn anisotropic exchange

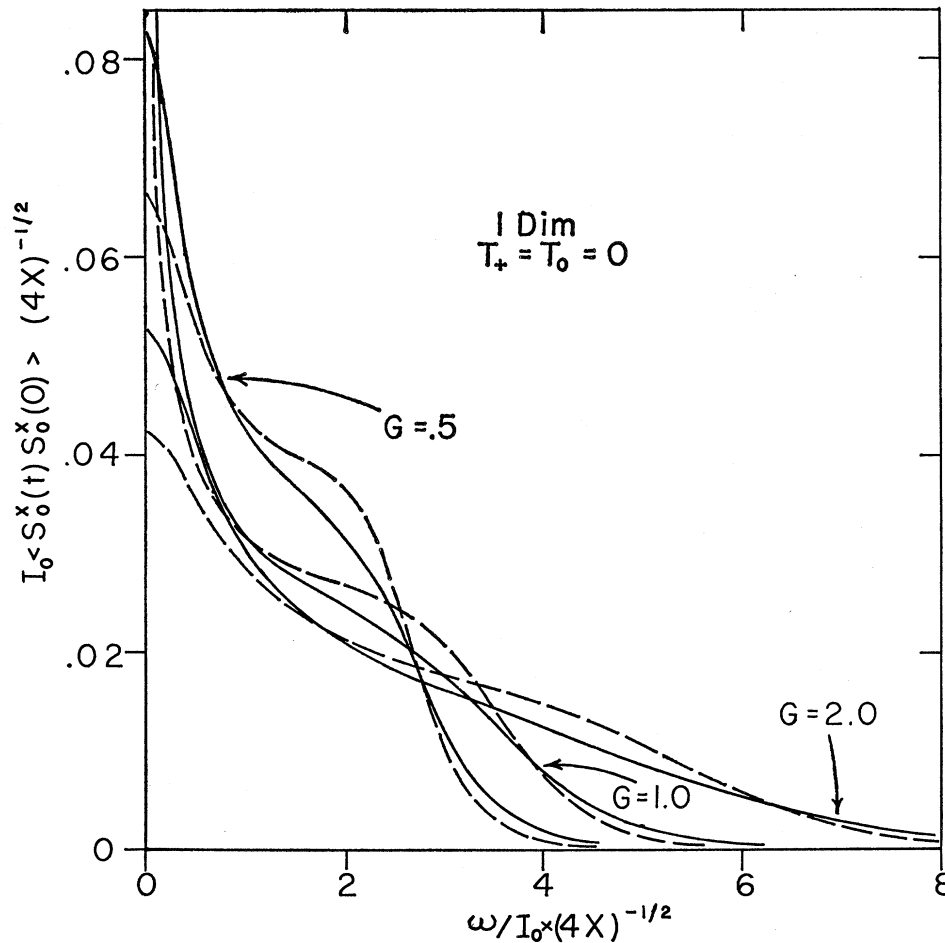


FIG. 11. Effect of anisotropy of the frequency spectrum of the dynamical transverse self-correlation function for a linear chain with only nn interactions and with spins  $\frac{1}{2}$  (dashed curves) and  $\infty$  (solid curves). Note that when the system is anisotropic, i.e.,  $G \neq 1$ , the frequency transform does not diverge at zero.

interactions, are as follows:

$$\langle \omega^2 \rangle_{\mathbf{K}^{zz}} = 2[4XI_0(1)]^2[(2-C_1)G^2 + 2(1-C_2)T_+^2], \tag{5.1a}$$

$$\begin{aligned} \langle \omega^4 \rangle_{\mathbf{K}^{zz}} / 256X^3I_0^4(1) &= 4G^2T_+(1-T_0)(2C_2-C_1) + 4[(C_1-2)G^2T_0 + (C_2-1)T_+^2] + \frac{2}{5}[(C_1-2)G^2 + 2(C_2-1)T_+^2T_0^2] \\ &+ 4[(2-C_1)G^2 + 2(1-C_2)T_+^2](1+T_0^2) - (8/5)[(2-C_1)G^4 + 2(1-C_2)T_+^4 + 20(G^2+T_+^2)^2] \\ &+ 3(C_1G^2 + 2C_2T_+^2)^2 - 16(C_1G^2 + 2C_2T_+^2)(G^2+T_+^2) + (10\bar{S})^{-1} \\ &\times [(C_1-2)(G^4 + \frac{3}{2}G^2) + 2(C_2-1)(T_+^4 + \frac{3}{2}T_+^2T_0^2)]; \end{aligned} \tag{5.1b}$$

$$\langle \omega^4 \rangle_{\mathbf{K}^{xx}} = 2[4\bar{S}I_0(1)]^2[-C_1G - 2C_2T_+T_0 + G^2 + T_+^2 + T_0^2 + 1], \tag{5.2a}$$

$$\begin{aligned} \langle \omega^4 \rangle_{\mathbf{K}^{xx}} / 256X^3I_0^4(1) &= \frac{1}{10}(X^{-1}+6)(-1-T_0^4 + 2C_1G^3 + 4C_2T_+^3T_0) \\ &+ (1/20)(X^{-1}+16)(C_1G + 2C_2T_+T_0^3 - 3G^2 - 3T_+^2T_0^2) - \frac{1}{4}(X^{-1}+4)(G^4 + T_+^4) \\ &+ 10(G^2 + T_+^2)^2 + 6(1+T_0^2)^2 - 8(C_1G + 2C_2T_+T_0)(1+T_0^2) + 3(C_1G + 2C_2T_+T_0)^2 \\ &+ 12(G^2 + T_+^2)(1+T_0^2) - 12(C_1G + 2C_2T_+T_0)(G^2 + T_+^2) \\ &+ GT_+[C_1(-2G^2 + 4 + 2T_0 + 2T_+) + C_2(-2GT_+ + 4G) - 4GT_0 - 8G] \\ &+ GT_0[C_1(-4 + 2G^2) + C_2(4G + 2GT_0)] - 4C_2T_+T_0. \end{aligned} \tag{5.2b}$$

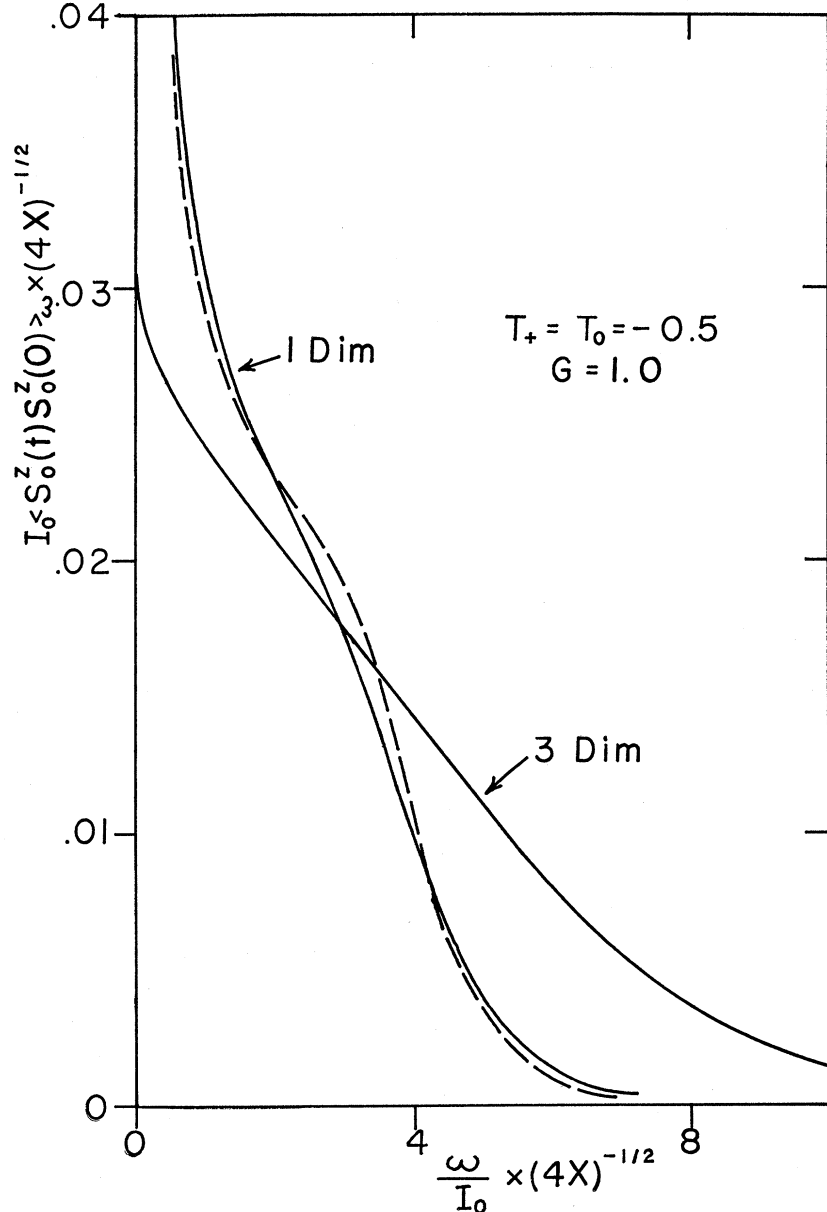


FIG. 12. Effects of the presence of second nn exchange on the frequency spectrum of the longitudinal self-correlation for a one-dimensional array of spins of magnitudes  $S = \frac{1}{2}$  (dashed curve) and  $S = \infty$  (full curve) and a three-dimensional (i.e., self-correlation) array with  $S = \infty$ . For simplicity, we have assumed isotropic exchange with second-neighbor exchange being one-half as large as the nn exchange and of opposite sign. With the increase in the range of the interaction, the somewhat improved agreement with a law of "corresponding states" (shown here for the one-dimensional lattice) should be noted. In fact, the  $S = \frac{1}{2}$  curve for the simple cubic lattice is too close to the  $S = \infty$  curve to be plotted.

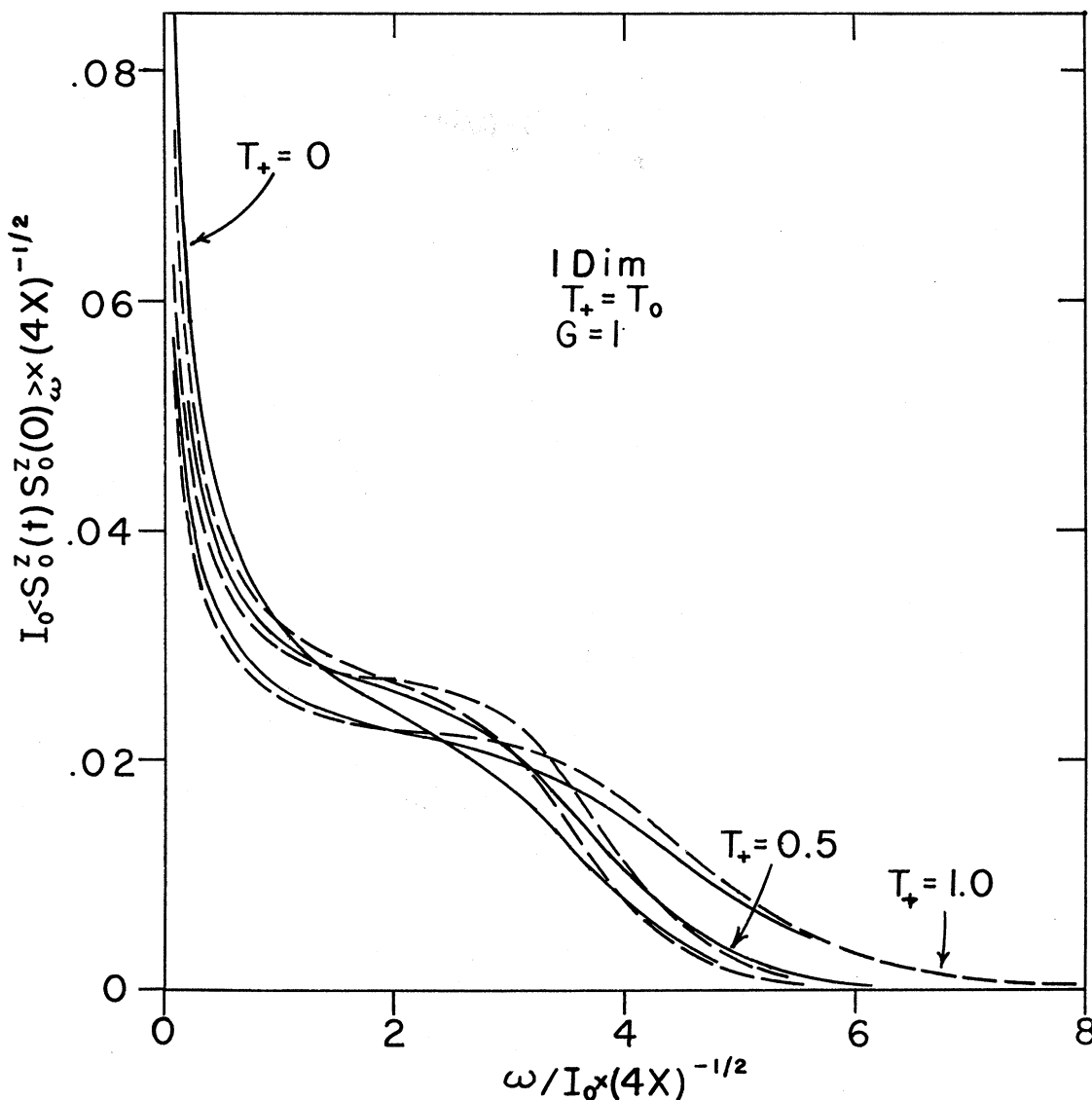


FIG. 13. Effects of the size of the nnn exchange on the frequency spectrum of the longitudinal self-correlation function. For simplicity, we have assumed isotropic exchange. The relevant spin system is one-dimensional with  $S = \frac{1}{2}$  (dashed curves) and  $S = \infty$  (solid curves). The ratio of the nnn exchange to  $I_0(1)$  is denoted as  $T_+ = T_0$ . A comparison of the corresponding curves for  $S = \frac{1}{2}$  and  $S = \infty$  indicates the following general trends: (1) The frequency spectrum extends to larger frequencies with the increase in the strength of the nnn exchange relative to the nn exchange, and (2) the law of corresponding states holds more accurately as the relative strength of the nnn exchange increases.

Here, we have redefined  $C_1$  and  $C_2$  to be

$$C_1 = \cos(K_x) + \cos(K_y), \quad C_2 = \cos(K_x) \cos(K_y). \quad (5.3)$$

This given format of the moments  $\langle \omega^{2n} \rangle_K^{\alpha\alpha}$  is suitable for the study of cases where  $I_0(1)$  is nonvanishing. For the few particular cases, when  $I_0(1)$  is vanishing, we reformulate the moments in terms of another parameter  $H = I_+(2)/I_+(1)$ .

#### A. XY Limit

Analogously to the linear chain, an appropriate XY limit can also be defined in a two-dimensional system.

However, in contrast to the situation in one dimension, no exact solutions corresponding to the restricted XY model can be obtained in two dimensions. It is interesting, nevertheless, to investigate the dynamical properties of the two-dimensional model and to compare it with the corresponding results for a linear chain as well as those for other less anisotropic two-dimensional spin systems.

The results for the frequency Fourier transform of the longitudinal self-correlation for spins  $S = \frac{1}{2}$  and  $S = \infty$  are given in Fig. 3 for the case of nn exchange only. These results when plotted in the reduced scale



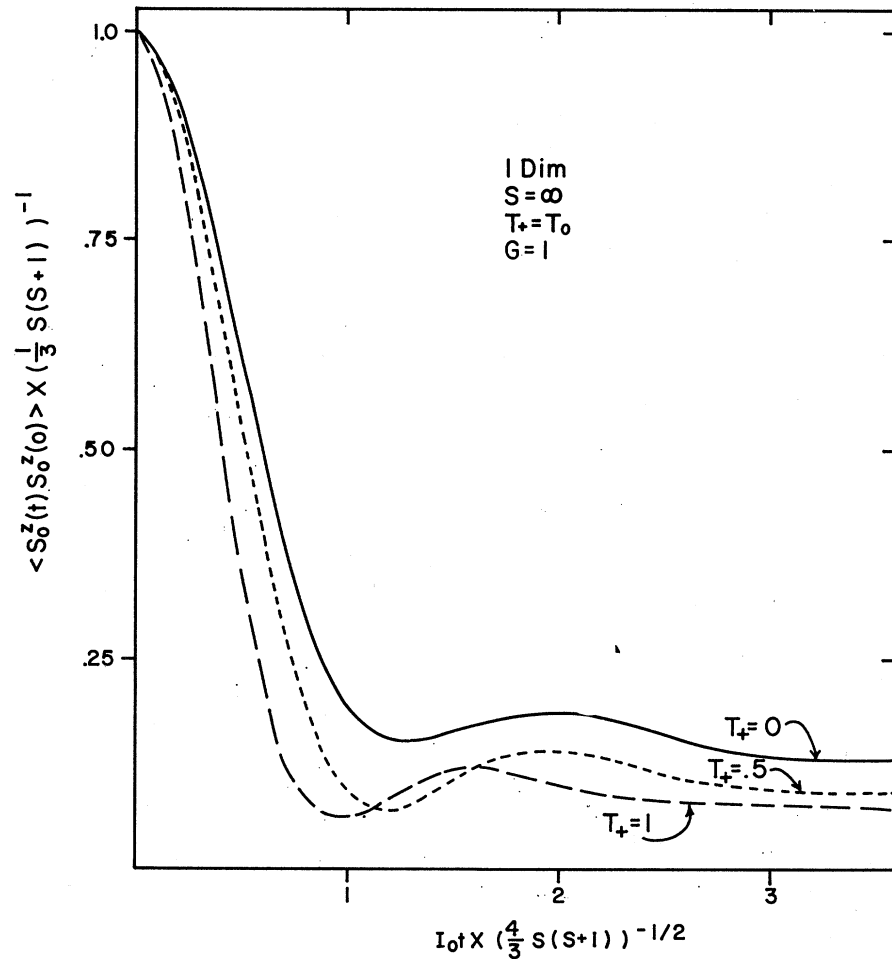


FIG. 14. Effects of the presence of longer-range exchange interactions are demonstrated upon the time dependence of the longitudinal self-correlation function. This plot refers to a linear chain of  $S = \infty$  spins with isotropic exchange. The parameters  $T_+ = T_0$  refer to the ratio of the nnn exchange to the nn exchange. With the increase in the relative magnitude of the nnn exchange, the rate of initial decay of the self-correlation is seen to increase gradually. Otherwise, the qualitative aspects of the time dependence remain largely unaffected.

seem, to a good approximation, to be spin-independent. As conjectured earlier, the discrepancy between the curves for  $S = \frac{1}{2}$  and  $S = \infty$  is smaller in two dimensions than in one. Moreover, the cutoff frequency is higher in two dimensions than in one and the cutoff is also somewhat less sharp.

The effects of the increase in the range of the exchange interaction are displayed in Fig. 6. On comparison with Fig. 5, which gives the corresponding results for one dimension, one notes that the qualitative effects of the increase in the range of the exchange interaction are similar to those of the increase in dimensionality.

The corresponding results for the transverse correlation are given in Fig. 7. Here again, differences are observed between the results for one and two dimensions. The zero-frequency transform is smaller in two dimensions and the magnitude of the cutoff frequency is bigger. Similarly, the comparison of various curves in Fig. 7 again verifies the general observation that the law of corresponding states is followed more closely in two dimensions than in one.

### B. General Anisotropic Case

Let us consider next the situation with more general spin interactions. Again, it is convenient to examine the case with only the nn exchange first. The results for the frequency spectrum of the longitudinal self- and nn correlations are plotted in Figs. 15 and 16. The frequency spectrum of the transverse self-correlation is depicted in Fig. 17. The structure of the longitudinal frequency spectrum again possesses many of the features observed in the one-dimensional case. These are (1) the Fourier transforms of all the longitudinal correlations diverge in the limit of zero frequency, (2) with the increase in the anisotropy, the frequency spectrum gradually takes on the features of the corresponding XY model, and (3) when the relative magnitude of the transverse exchange to the longitudinal exchange is decreased, the power spectrum of the longitudinal correlations narrows toward the origin. In the limit that this ratio is zero (i.e., in the nondynamical Ising-model limit), the corresponding spectrum will be a Dirac  $\delta$  function at the origin.

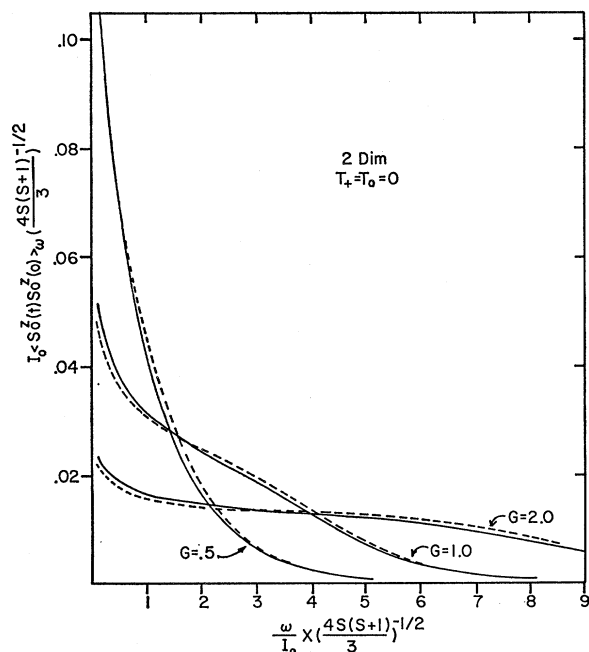


FIG. 15. Frequency spectrum of the longitudinal self-correlation for a two-dimensional square net with only nn exchange. The relative sizes of the transverse exchange and the longitudinal exchange is indicated by  $G = I_+(1)/I_0(1)$ . The dashed and the solid curves are for  $S = \frac{1}{2}$  and  $S = \infty$ , respectively. In the limit of zero frequency, the Fourier transform again diverges for all  $G$ . The rate of divergence, however, is weaker than for the corresponding cases in one dimension (compare Fig. 8). The discrepancy between the dashed and the full curves is, however, smaller in two dimensions than in one. Lastly, the cutoff frequency is higher in two dimensions than in one.

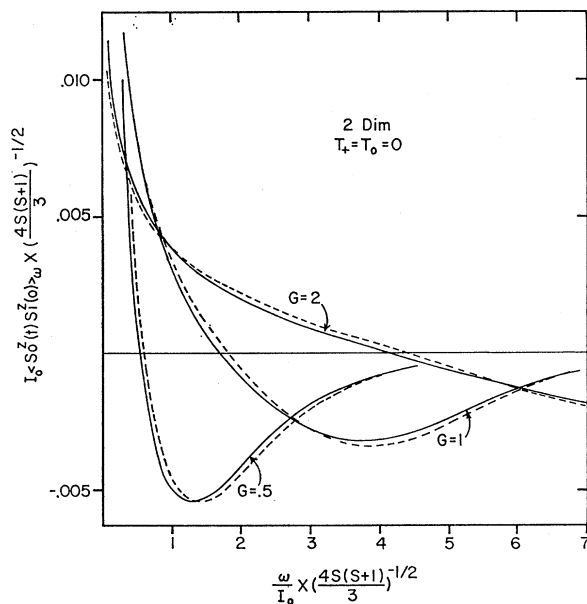


FIG. 16. Same as in Fig. 10, except that this case refers to two dimensions. The general trend noted elsewhere is also clear here, i.e., (1) the divergence of the zero-frequency transform is weaker in two dimensions than in one, and (2) the spectrum is spread towards somewhat higher frequencies in two dimensions.

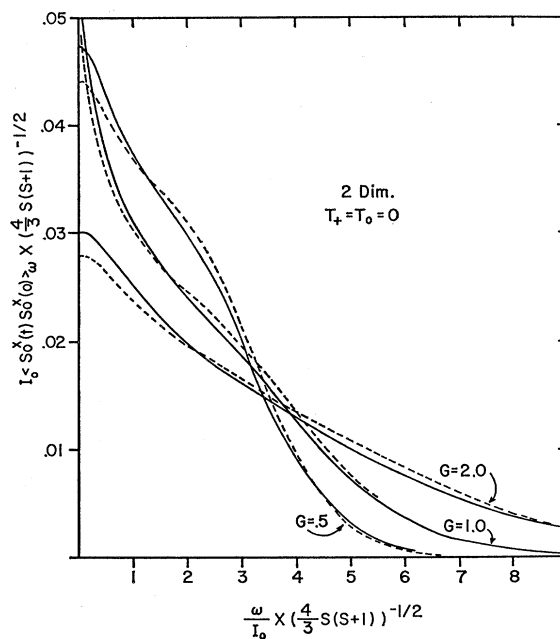


FIG. 17. Effect of anisotropy on the frequency spectrum of the transverse self-correlation function in two dimensions. The relative anisotropy of the nn exchange is denoted by  $G$ . All further neighbor exchange is assumed to be zero. These results should be compared with the corresponding results for one-dimensional systems given in Fig. 11. Here, the dashed and the solid curves refer to  $S = \frac{1}{2}$  and  $S = \infty$ , respectively. The relative magnitudes of the zero-frequency transforms should be compared with those for a linear chain. In the isotropic limit, i.e.,  $G = 1$ , these transforms are divergent. The relative divergence is, however, weaker in two dimensions than in one.

The differences between the corresponding frequency spectra for one- and two-dimensional cases are also similar to those already noted above in the case of the one- and two-dimensional XY models. For given value of the anisotropy, the spectrum is spread toward somewhat higher frequencies in the case of two dimensions, as compared to the corresponding spectrum for the linear chain. Similarly, the divergence for zero frequency is weaker for two dimensions than for one. Lastly, when the curves are plotted in the reduced frequency scale, the relative discrepancy between different spins is smaller for the two-dimensional lattice than for the linear chain.

The behavior of the frequency Fourier transform of the transverse correlation function, for two and one dimensions, also possesses analogous features. Except for the isotropic limit, i.e.,  $G = 1$ , the Fourier transform is finite at the origin. The relative magnitudes of the zero-frequency transforms are smaller in two dimensions than in one dimension. Similarly, the cutoff frequency is larger in two dimensions. Finally, the relative accuracy of the law of corresponding states increases in two dimensions as compared to one dimension.

Finally, in order to examine the effects of the increase in the range of interaction, we have plotted in Fig. 18 the frequency Fourier transform of the longitudinal

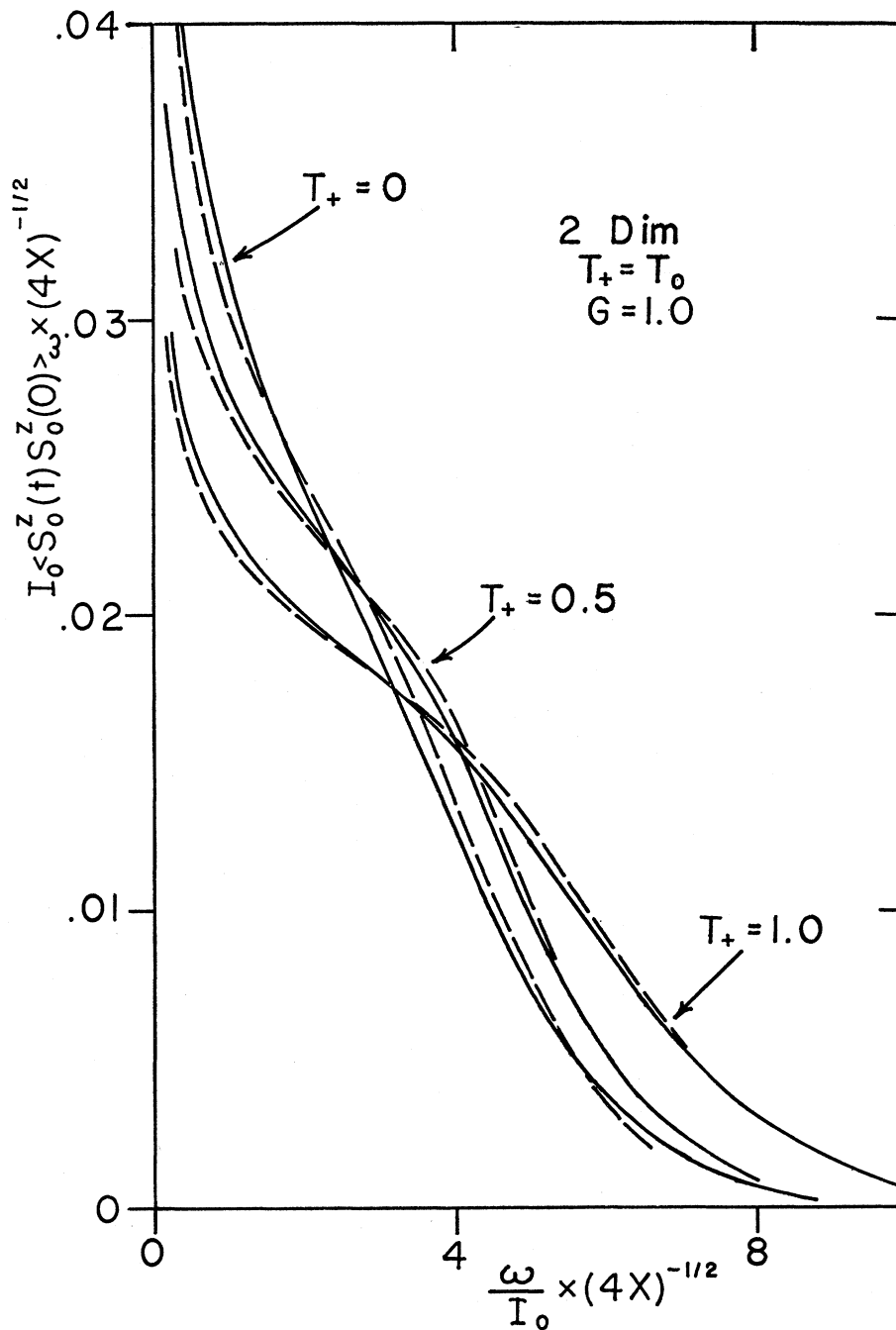


FIG. 18. Effects of the size of the nnn exchange on the frequency spectrum (plotted in the reduced units) of the longitudinal self-correlation function for a two-dimensional square net. For simplicity, we have assumed isotropic exchange. The dashed and solid curves refer to the case of  $S = \frac{1}{2}$  and  $S = \infty$ , respectively. The ratio of the nnn to the nn exchange is denoted as  $T_+ = T_0$ . To get a feel for the effects of the increase in dimensionality, compare with Figs. 16 and 17, which refer to the linear chain, and with Fig. 26, which refers to the three-dimensional simple cubic) lattice.

self-correlation function for a system with isotropic exchange. These results should be compared with the corresponding results for the linear chain given in Fig. 13. It is clear that the increase in dimensionality and the increase in the relative magnitude of the nnn exchange affect the results in the same general direction, i.e., they both cause a better fit of the corresponding results for different spins (when plotted on a reduced scale). Moreover, they both cause the frequency spec-

trum to spread out toward higher frequencies and thereby to increase the magnitude of the cutoff frequency.

### VI. RESULTS IN THREE DIMENSIONS

For simplicity, we consider a simple cubic lattice. The units of length are chosen such that the cube edge is of length unity. With only nn and nnn exchange inter-

actions, the various moments are as follows:

$$\langle \omega^2 \rangle_{\mathbf{K}^{zz}} = 2[4XI_0(1)]^2[(3-C_1)G^2 + 2(3-C_2)T_+^2], \tag{6.1a}$$

$$\begin{aligned} \langle \omega^4 \rangle_{\mathbf{K}^{zz}} / 256X^3I_0^4(1) &= 8(C_2-C_1)G^2T_+(1-T_0) + 8(C_1-3)G^2T_0 + 4(C_2-3)T_+^2(1+2T_0^2) \\ &+ \frac{2}{5}[(C_1-3)G^2 + 2(C_2-3)T_+^2T_0^2] + 6[(3-C_1)G^2 + 2(3-C_2)T_+^2](1+2T_0^2) \\ &- (8/5)[(3-C_1)G^4 + 2(3-C_2)T_+^4] + 45(G^2+2T_+^2)^2 + 3(C_1G^2+2C_2T_+^2)^2 - 24(C_1G^2+2C_2T_+^2) \\ &\times (G^2+2T_+^2) + (10\bar{S})^{-1}\{(C_1-3)[G^4+\frac{3}{2}G^2] + 2(C_2-3)(T_+^4+\frac{3}{2}T_+^2T_0^2)\}; \end{aligned} \tag{6.1b}$$

$$\langle \omega^2 \rangle_{\mathbf{K}^{xx}} = 2[4XI_0(1)]^2[-C_1G-2C_2T_+T_0+\frac{3}{2}(G^2+1)+3(T_+^2+T_0^2)],$$

$$\begin{aligned} \langle \omega^4 \rangle_{\mathbf{K}^{xx}} / 256X^3I_0^4(1) &= (3/20)(X^{-1}+6)[-1-2T_0^4+\frac{4}{3}C_1G^3+(8/3)C_2T_+^3T_0] \\ &+ (1/20)(X^{-1}+16)[C_1G+2C_2T_+T_0^3-\frac{9}{2}G^2-9T_+^2T_0^2]-\frac{3}{8}(X^{-1}+4)(G^4+2T_+^4) \\ &+ (27/2)(1+2T_0^2)^2 + (45/2)(G^2+2T_+^2)^2 - 12(C_1G+2C_2T_+T_0)(1+2T_0^2) + 3(C_1G+2C_2T_+T_0)^2 \\ &+ 27(G^2+2T_+^2)(1+2T_0^2) - 18(C_1G+2C_2T_+T_0)(G^2+2T_+^2) + GT_+[4C_1(2-G^2+T_++T_0) \\ &+ 2C_2G(2-T_+)-12G(T_0+2)] + GT_0[4C_1(-2+G^2)+2C_2G(2+T_0)] \\ &+ 4C_2T_+(-T_+^3-T_0-2T_0^3+3T_+T_0^2+2T_+^2T_0) - 24T_+^3T_0. \end{aligned} \tag{6.2b}$$

Here we have redefined  $C_1$  and  $C_2$  to be

$$\begin{aligned} C_1 &= \cos K_x + \cos K_y + \cos K_z, \\ C_2 &= \cos K_x \cos K_y + \cos K_x \cos K_y + \cos K_y \cos K_z. \end{aligned} \tag{6.3}$$

**A. XY Limit**

As before, we shall first examine the XY limit. With the added simplification of nn (transverse) exchange

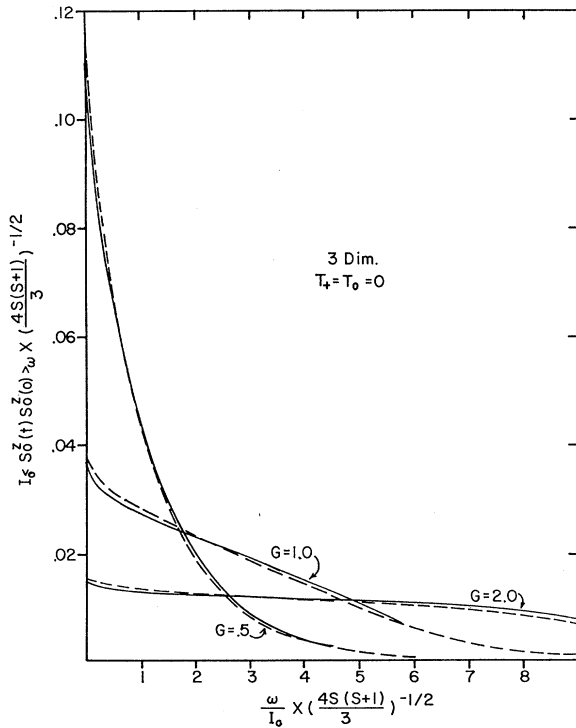


FIG. 19. Plot shows the effects of anisotropy, as well as the dependence on the magnitude of the spins, of the frequency Fourier transform of the longitudinal self-correlation for a three-dimensional (simple cubic) lattice with only nn exchange. The anisotropy parameter as usual denotes the ratio of  $I_+(1)$  to  $I_0(1)$ . The solid and dashed curves refer to spin  $\frac{1}{2}$  and spin  $\infty$ , respectively.

only, we have plotted the results for the frequency Fourier transform of the longitudinal self-correlation in Fig. 3.

The examination of Fig. 3 reveals some of the same general features already noted for the corresponding results in one and the two dimensions. The increase in the dimensionality to 3, however, has one important difference. The zero-frequency Fourier transform of the longitudinal correlation functions is now no longer divergent.

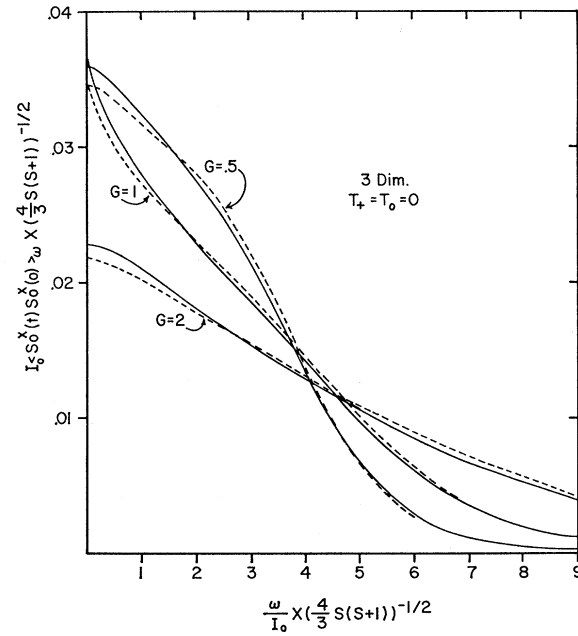


FIG. 20. Effect of anisotropy and the spin magnitude on the frequency Fourier transforms of the transverse self-correlation of a three-dimensional (simple cubic) lattice with only nn exchange. The solid and dashed curves refer to  $S = \infty$  and  $S = \frac{1}{2}$ , respectively. The effects of dimensionality are obvious from a comparison with the corresponding results for a linear chain (see Fig. 11) and a two-dimensional square net (Fig. 17).

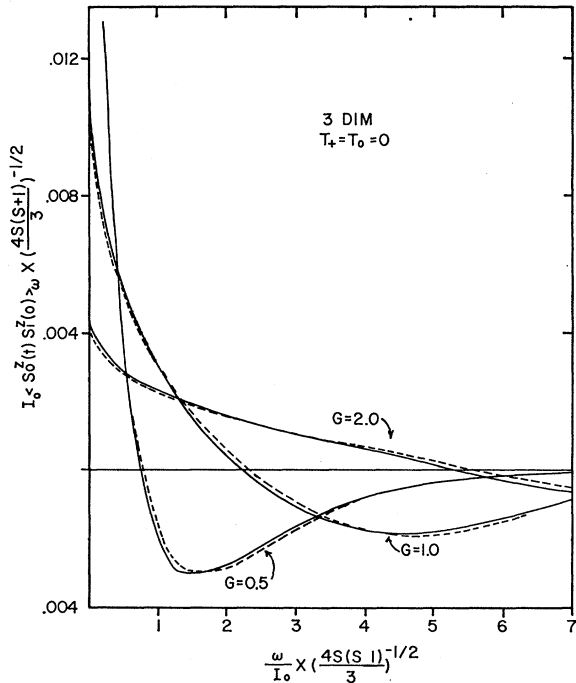


FIG. 21. Frequency Fourier transform of the nn longitudinal correlation function for a three-dimensional (simple cubic) lattice with only nn exchange. The dashed and solid curves, respectively, relate to  $S = \frac{1}{2}$  and  $S = \infty$ . To get a feel for the effects of dimensionality, these curves should be compared with the corresponding ones for one dimension (Fig. 10) and two dimensions (Fig. 16).

**B. General Anisotropic Case**

Beginning with the simple case of nn exchange only, we have plotted the frequency Fourier transform of the longitudinal correlation function in Fig. 19, the transverse self-correlation function in Fig. 20, and the longitudinal nn correlation in Fig. 21. In the low-frequency regime, the structure of the results for the longitudinal case is in marked contrast with the corresponding results in one and two dimensions. For given anisotropy  $G$ , the spectrum is now finite in the limit of zero frequency (except, of course, for the trivial case  $G=0$  when the system reduces to a nondynamical Ising model for which the frequency spectrum degenerates into a Dirac  $\delta$  function centered at the origin). In other respects, the results follow the established pattern: Namely, that, for given value of the anisotropy  $G$ , the frequency spectrum is extended towards higher frequencies as the dimensionality is increased, and for given dimensionality, the structure gradually approaches that for the  $XY$  limit or the Ising limit according to whether the anisotropy  $G$  is increased or decreased from the isotropic value  $G=1$ .

To check the above statement regarding the effects occasioned by the increase in the range of the exchange interaction, we have plotted the frequency Fourier

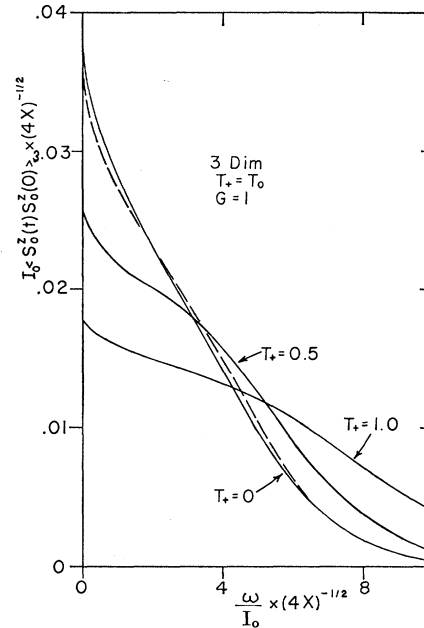


FIG. 22. Effect of the increase in the range of the exchange interactions of the frequency spectrum of the longitudinal self-correlation function for a three-dimensional (simple cubic) lattice. For simplicity, we have assumed isotropic exchange. The dashed curve is for  $S = \frac{1}{2}$  and the solid curves for  $S = \infty$ . The other spin- $\frac{1}{2}$  curves are too close to the corresponding spin- $\infty$  curves to be plotted conveniently. The effects of dimensionality can be observed by comparison with Fig. 12, for the linear chain, and Fig. 18, for the two-dimensional square net.

transform of the longitudinal self-correlation function in Fig. 22. Again, the trend noted is confirmed.

Similarly, to verify the above mentioned statement regarding the effects of dimensionality, we have displayed the time dependence of the longitudinal self-correlation function (with only the isotropic nn exchange) in Fig. 23. The results are, again, in accord with the general tenor of the statement given above.

Finally, it is interesting to examine the behavior of the rate at which the magnetization density diffuses, i.e.,  $D^{zz}$ . Within the framework of the phenomenological approximation used in the present paper, this yields, for nn exchange only,

$$D^{zz} = 2G^2 I_0 \left( \frac{\pi X}{28/5 - 3/20X + G^2(52/5 - 1/10X)} \right)^{1/2} \quad (6.4)$$

This result should be compared with that obtained by the use of a truncated integral equation procedure [for this comparison, see Ref. 17, Eq. (8)]. The parameter  $a$  in this equation should be put equal to unity ( $z=6$  and  $\gamma$  equal to the  $G$  of the present paper), i.e.,

$$D^{zz} = (2\pi X/3)^{1/2} G^2 I_0 / (1+G^2)^{1/2} \quad (6.5)$$

<sup>17</sup> R. A. Tahir-Kheli, J. Appl. Phys. 40, 1550 (1969).

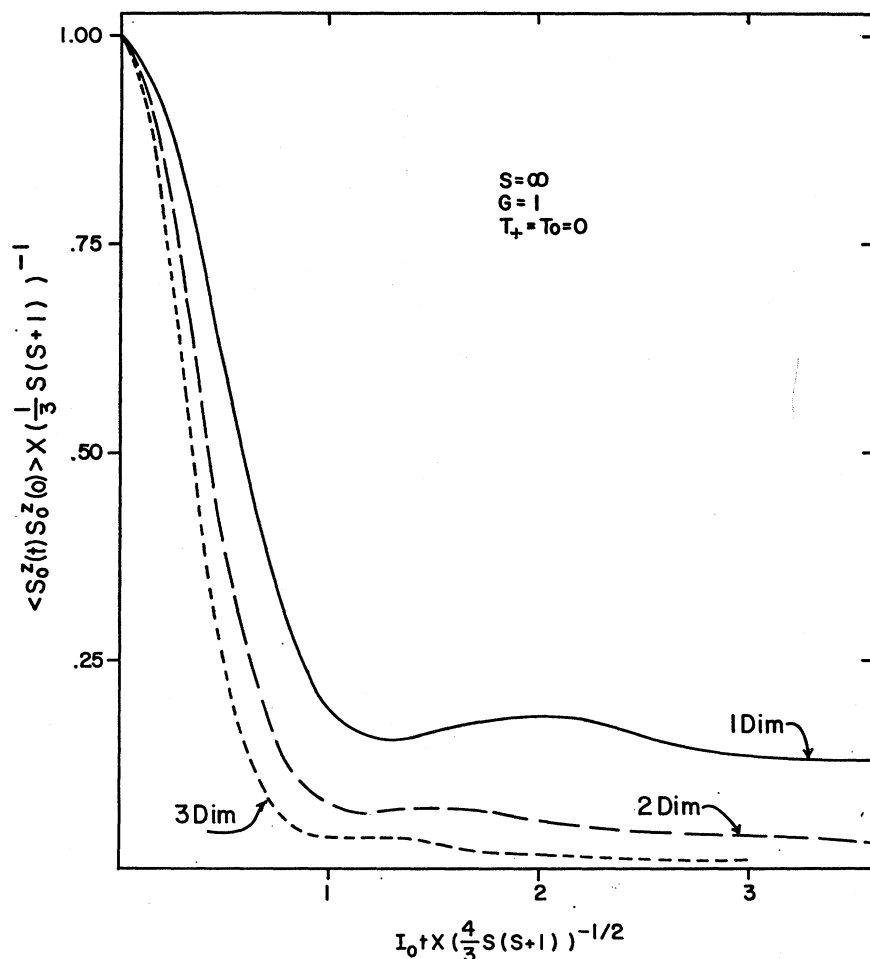


FIG. 23. Effects of dimensionality on the time dependence of the longitudinal self-correlation function. The curves are drawn for the limiting case of spin  $\infty$ . For simplicity, the exchange is taken to be isotropic and its range is limited to the nn distance. The relaxation time (in which the correlation falls off to half its original magnitude) is seen to be a strong function of the dimensionality: it being shorter the higher the dimensionality. Otherwise, the general structure of the results is seemingly not a strong function of the dimensionality. Note that this result agrees with the heuristic conjecture that to a rough approximation the effects of the increase in dimensionality are analogous to the results of an increase in the effective range of the exchange interactions.

## VII. CONCLUSIONS

In this paper, we have evaluated the zeroth, second, and fourth frequency moments of the frequency-wave-dependent spectral functions for anisotropic Heisenberg spin systems in the limit of elevated temperature. Our expressions are valid for all spins for arbitrary range of the exchange interactions and for arbitrary dimensionality.

We then specialized these expression to the case of one-, two-, and three-dimensional systems and considered only the nn and nnn exchange. We constructed a phenomenological representation of the generalized diffusivity such that the exactly calculated frequency moments were automatically preserved for all wave vectors. With this representation, we computed the frequency- (and sometimes also wave-vector) dependent Fourier transforms of the longitudinal and transverse correlations. We conducted detailed examination of the

predictions of our approximate theory for the exactly soluble model, i.e., one-dimensional  $S = \frac{1}{2}$  XY model with only nn exchange. We found that our approximate theory gave qualitatively satisfactory representation of the space-time-dependent correlations in the system where exact results are known.

In view of our previous observations<sup>11</sup> that such a theory also gives similarly satisfactory representation of the correlations for some limiting cases of isotropic Heisenberg systems,<sup>3-7</sup> we may hope that the present results are equally meaningful for all the various intermediate cases for which reliable solutions are not available.

## ACKNOWLEDGMENT

We are greatly indebted to the Temple University computer center for generous allotment of computer time on their CDC-6400.